Aus der medizinischen Universitäts- und Poliklinik Tübingen

**Abteilung Innere Medizin VIII,
Klinische Tumorbiologie**

Evaluation of a novel epi-virotherapeutic treatment strategy of pancreatic cancer combining the oral histone deacetylase inhibitor resminostat with oncolytic measles vaccine virus

**Dissertation
zur Erlangung des Doktorgrades
der Medizin**

**der Medizinischen Fakultät
der Eberhard Karls Universität
zu Tübingen**

vorgelegt von

Ellerhoff, Tim Patrick

2017

Dekan: Professor Dr. I. B. Autenrieth

1. **Berichterstatter: Professor Dr. U. Lauer**
2. **Berichterstatter: Professor Dr. M. Schindler**
3. **Berichterstatter: Professor Dr. M. Möhler**

Datum der Disputation: 19.06.2017

Content

1. Introduction

1.1. Pancreatic Cancer

1.1.1. Epidemiology

Pancreatic cancer still is one of the tumor entities with the highest mortality rate. Less than 5% of the patients with pancreatic cancer survive more than five years (Hidalgo, 2010). According to the cancer statistics in 2013, there were approximately 43,920 new-onset pancreatic cancer cases in the USA, with 37,290 deaths (Siegel et al., 2013). The most common histologic type of pancreatic cancer is pancreatic ductal adenocarcinoma (PDAC), representing 95% of pancreatic tumors (Tanaka, 2015). Risk factors can be divided into two major groups, one consisting of a chronic inflammation due to chronic pancreatitis, tobacco smoking or alcohol, the other of diet factors such as hyperglycaemia, obesity and diabetes mellitus (Maisonneuve and Lowenfels, 2015).The poor prognosis results mainly from a late diagnosis and a lack of therapy approaches with curable intention. Since most patients do not develop any specific symptoms at early stages of the disease and there are moreover no reliable screening tests, metastases have often already occurred at the time point of diagnosis (Rao and Mohammed, 2015, Garrido-Laguna and Hidalgo, 2015).

1.1.2. Established therapies

The only available therapy with curative intention to date is the complete surgical resection. Nonetheless, patients undergoing surgical interventions have miserable prospects of long-term-survival. 85% of operated patients develop locoregional recurrences or distant metastases over the course of time (Sutton and Abbott, 2014).

Since surgery is associated with bad outcomes, almost all patients receive chemotherapeutics afterwards. Beyond application in an

adjuvant setting, cytotoxic drugs are furthermore applied in neo-adjuvant settings as well as in palliative stages of disease (Garrido-Laguna and Hidalgo, 2015). Whereas 5-fluorouracil (5-FU) had been the only beneficial agent for decades, it has been replaced by gemcitabine in the late 90s (Burris et al., 1997). Other chemotherapy based regimes, like FOLFIRINOX (5-FU, leucovorin, irinotecan, and oxaliplatin) and gemcitabine plus nab-Paclitaxel provide, if any, a few months improvement in survival (Conroy et al., 2011, Mohammed et al., 2014).

Regarding the failure of chemotherapeutics in pancreatic cancer, several resistance mechanisms have been revealed. In particular, overexpression of certain drug efflux pumps (ABC transporter) and enzymes that cleave drugs like gemcitabine, specific genetic mutations as well as deregulation of key signaling pathways like the NF-κB and Notch pathway were shown causing chemo-resistance (Long et al., 2011). Constituting another big obstacle, chemotherapeutics have to overcome the distinctive hypoxic, acidic environment in pancreatic cancer that is characterized by an insufficient vascularization, thereby impairing drug delivery especially in the center of solid tumors (Long et al., 2011). Concerning the tumor environment, pancreatic cancer is typically pervaded by a dense desmoplastic tissue. Therein, extracellular matrix (ECM) proteins are produced that protect cancer cells from the induction of apoptosis by anticancer drugs (Miyamoto et al., 2004).

1.1.3. Molecular-targeted therapy

With the growing understanding of molecular pathways involved in pancreatic cancer, new therapeutic targets have been identified. Erlotinib, an Epidermal Growth Factor Receptor tyrosine kinase inhibitor (EGFR-TKI), in combination with gemcitabine was approved by the U.S. Food and Drug Administration (FDA) for the

treatment of locally advanced and metastatic pancreatic cancer in 2005, extending the median survival time from 5.91 to 6.21 months (Steins et al., 2014). The most common mutation in pancreatic cancer concerns KRAS, being present in 90% of tumor cells. This cornerstone of carcinogenesis in pancreatic cancer might provide a possible beneficial effect of ras inhibitors. Unfortunately, several farnesyltransferase inhibitors which are involved in post-translational modifications of ras proteins, failed to kill tumor cells successfully (Teague et al., 2015). Likewise, approaches inhibiting proteins downstream in the ras pathway, like MEK, were not successful (Garrido-Laguna and Hidalgo, 2015). Eventually, a combination of gemcitabine with the anti-VEGF monoclonal antibody Bevacizumab did not yield promising results in a randomized phase III study either (Kindler et al., 2010).

Further innovative approaches are being evaluated at the moment, including the CTLA-4 inhibitor Ipilimumab, tumor vaccines and tumor specific antibodies (Teague et al., 2015).

This short overview about present strategies to treat pancreatic cancer outlines established therapies as well as new approaches being currently tested, in sum demonstrating the urgent demand for novel effective therapeutic strategies in pancreatic cancer.

1.2. Oncolytic virotherapy

The term oncolytic virotherapy describes the use of viruses as anticancer agents. Due to their naturally occurring or genetically modified ability to selectively replicate in and afterwards lyse tumor cells, healthy tissue remains unaffected.

1.2.1. History of discovery and research

Already in the mid-1800s, case reports that described tumor regressions of cancer patients suffering from virus infections at the same time, emerged (Kelly and Russell, 2007). For this reason

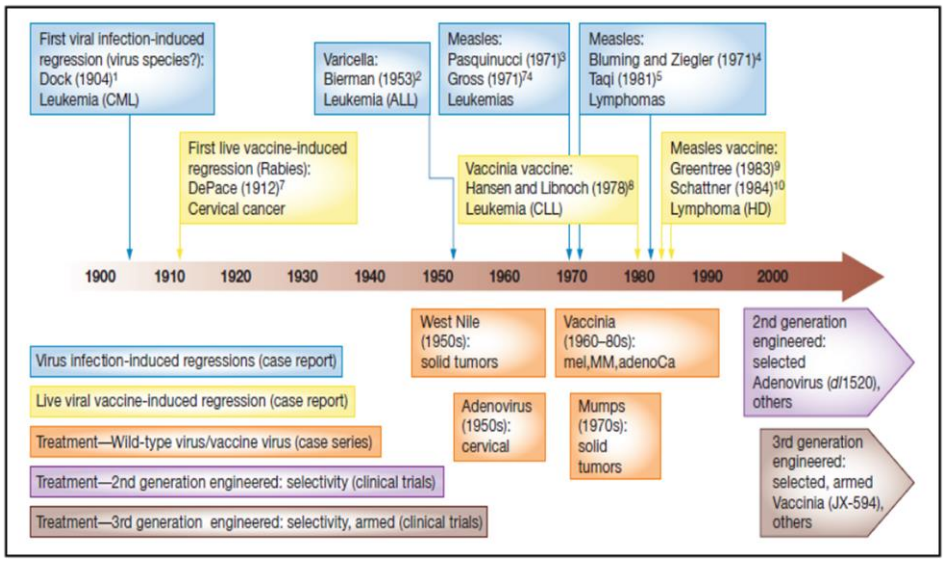

Figure 1: Timeline of the clinical history of virotherapy; taken from (Liu et al., 2007)

George Dock assumed that infections can be utilized in order to cure cancer patients (Hammill et al., 2010). In line with this, clinicians attempted to conquer cancer with the aid of body fluids obtained from virus infected people (Southam, 1960). Similar observations of tumor regression were made following anti-rabies vaccination (Moore, 1954) (Fig. 1). Initially, wild-type viruses were used and consequently lots of infectious complications occurred. After having exploited recombined DNA technology to create attenuated viruses, virotherapy has finally made its breakthrough in becoming a well-respected alternative as compared to other ant-cancer drugs (Hammill et al., 2010).

After having gained more and more knowledge about different tumor entities and their pathological features, it became evident that haematological malignancies are especially susceptible to virus-mediated oncolysis. In this regard, infection with measles virus induced remission of Hodgkins´s Lymphoma (Taqi et al., 1981) and Burkitt´s Lymphoma (Bluming and Ziegler, 1971) (Fig.1). The astonishing response rate of these malignancies can be ascribed to the concomitant immune suppression preventing systemic elimination of viruses in the blood stream (Liu et al., 2007).

Moreover, oncolytic viruses have shown promising effectivity in the treatment of solid tumors. Since many in vitro studies had provided new insights into mechanisms of action, several clinical studies have been performed. In this context, different oncolytic viruses have been proven to be efficient in the treatment of sarcomas (Lettieri et al., 2012), pancreatic cancer (Wennier et al., 2011) and glioblastoma multiforme (Wollmann et al., 2012).

1.2.2. Mechanism of action

Since viruses are not capable of replicating themselves like living organisms, they have to exploit the synthetic machinery of their host cells. After having produced a great number of new virions, host cells undergo cell lysis, subsequently releasing viruses, which in turn spread from cell to cell, thereby infecting the nearby tissue and proceeding the infection in a self-amplified manner (Giorda and Hebert, 2013).

As commonly known, each virus yields a distinct tropism for specific cells. Fortunately, several viruses naturally exhibit a selective tropism for different cancer cells, e.g. parvovirus, reovirus, newcastle disease virus, mumps virus and moloney leukemia virus. Other viruses were shown to be well suited for genetic modifications (Russell et al., 2012)(Fig. 1). Typical strategies are engineering viruses to target specific surface proteins as entry receptors or to express their genes under the control of tumor specific promoters (Russell et al., 2012). Another reason for cancer cell tropism is a lack in the antiviral response, being initiated by type I Interferon signaling. Whereas normal cells manage to efficiently eliminate invaded viruses, approximately 80% of cancer cells exhibit mutations in this pathway (Stojdl et al., 2003). More precisely, healthy cells detect non-self-associated molecular patterns (PAMPs) by means of pattern recognitions receptors (PRRs). As a consequence, viral nucleic acid or specific viral surface proteins are

identified, resulting in the induction of type I IFN production in infected cells. These cells as well as surrounding cells establish an antiviral state due to binding of IFN-β to its receptor. Therefore, they express antiviral enzymes, shut down their protein synthesis machinery in order to restrict viral replication and express additionally MHC-I proteins, whereby facilitating immune cells the detection of infected cells (Diamond and Farzan, 2013) (Fig. 2). In contrast to healthy cells, cancer cells do not express genes which encode for pathogen-receptors and antiviral effectors like RNAses and GTPases (Sen, 2001), making them an easy target for oncolytic viruses. Beyond that, cancer cells feature a resistance to apoptosis as well as to the ability of shutting down gene expression and translation which are naturally strategies to encounter virus infections (Russell et al., 2012).

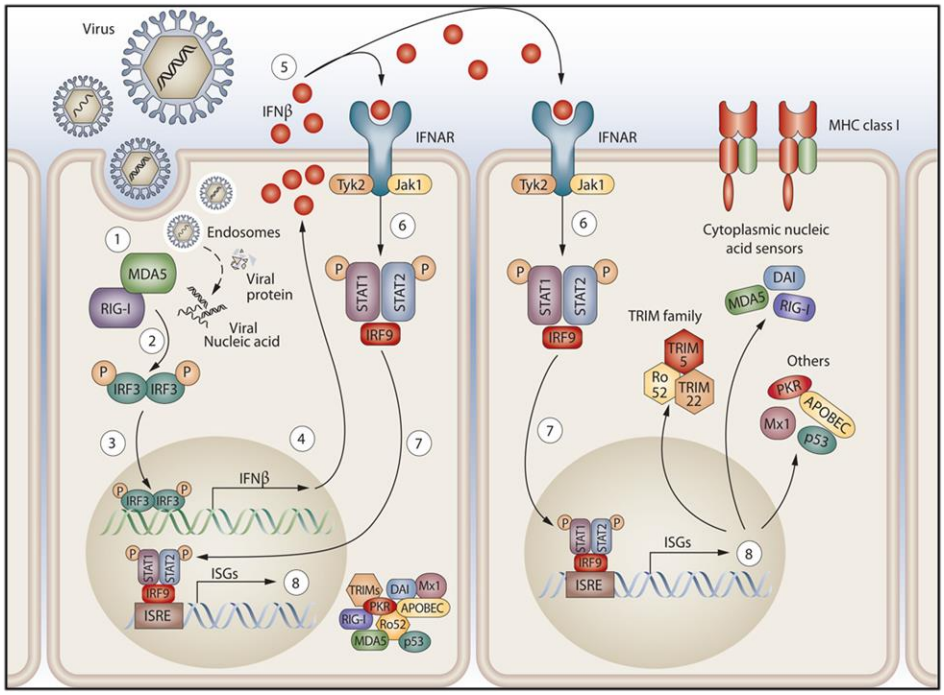

Figure 2: Type I IFN signaling following virus infection
After virus infection, cellular pathogen sensors (MDA5 and RIG-I) detect invaded viruses through their nucleic acid which is followed by phosphorylation of IRF3 and consequently the production of IFN-β (1-4). IFN-β takes effect in autocrine as well as paracrine manner, whereby binding to its receptor runs downstream JAK/STAT signaling (5-7). The complex of STAT 1, STAT 2 and IRF 9 initiates

the expression of IFN-stimulated genes (ISGs) (8); taken from Hall and al. (Hall and Rosen, 2010)

Furthermore, viruses display a perfect vector for delivering genes to cancer cells in order to potentiate the efficiency of oncolytic viro-therapy. Thus, genomes of different viruses can be modified by adding genes encoding for proteins that both directly and indirectly enhance their therapeutic effect. Typical strategies are inserting pro-apoptotic proteins like TRAIL (Tumor Necrosis Factor Related Apoptosis Inducing Ligand) or pro-drug convertases like supercytosine deaminase (Kasman et al., 2012, Lampe et al., 2013).

1.2.3. Oncolytic immunotherapy

The common way of identification and combat against mutated cells, mainly executed by antigen-presenting cells (APCs) and NK cells, is avoided through several mechanisms in tumors, evolved during the process of tumorigenesis. Important steps being frequently impaired are DC maturation, T cell extravasation by downregulation of adhesion molecules, overexpression of inhibitory receptors like PD-L1 and eventually by the downregulation of identification receptors such as MHC-I molecules (Zamarin and Wolchok, 2014). These barriers eventuate in an immunosuppressive tumor-microenvironment.

To further emphasize these observations, the extent of T cell infiltration into the tumor bed seems to be a good prognostic marker for the outcome of patients suffering from different cancer types and is momentary evaluated for embedding into the new “immunoscore” classification of cancers (Galon et al., 2012, Fridman et al., 2012).

Astonishingly, OVs were found being able to overcome those barriers. In this way, they are capable of changing the tumor microenvironment regarding the cytokine profile as well as the amount of expressed immunosuppressive receptors, thereby

attracting more and more immune cells to the tumor bed. Considering oncolysis, plenty of tumor associated antigens (TAAs) are released which are in turn detected by dendritic cells, following antigen presentation to lymphocytes and initiation of an anti-tumor immune response. Cancer cells can be additionally easier recognized due to upregulation of MHC-I molecules (Prestwich et al., 2009, Melcher et al., 2011, Woller et al., 2014, Lichty et al., 2014, Zamarin and Wolchok, 2014)(Fig. 3). These virus-induced processes enable a well-coordinated combat against tumors and therefore prompted researchers to change the classical term of "virotherapy" to "oncolytic immunotherapy" (Coffin, 2015).

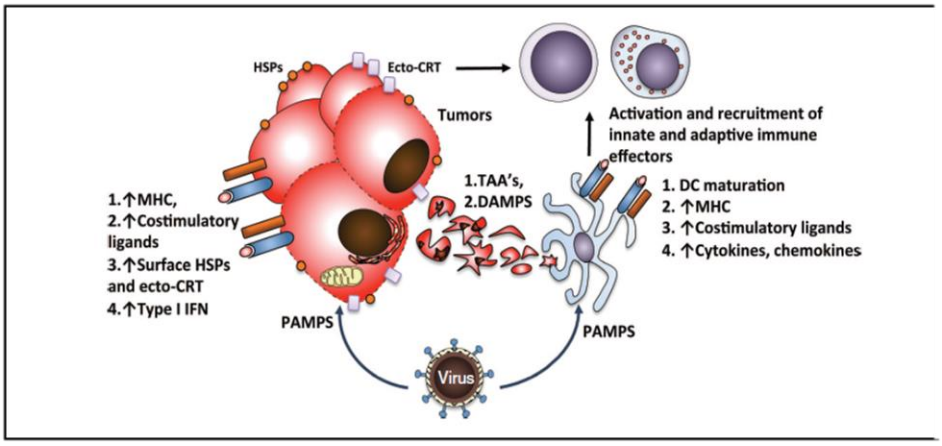

Figure 3: Principles of oncolytic immunotherapy

The schematic depiction shows the impact of virus infection on tumor cells, the cancer microenvironment and on immune cells. Oncolytic viruses induce expression of MHC-I molecules as well as costimulatory receptors in tumor cells. Through oncolysis, tumor- associated-antigens (TAAs) and damage-associated-molecular patterns (DAMPs) are exposed. Finally, this leads to an infiltration of immune cells in tumor tissue. Taken from (Zamarin and Wolchok, 2014).

1.2.4. Advantages and disadvantages

In contrast to established cancer therapeutics which affect the entire organism and are therefore associated with partly severe side effects like lymphopenia or anemia oncolytic viruses show little adverse drug reactions due to their relative cancer selectivity (Bourke et al., 2011). Moreover, only a single dose is required for eliciting amazing effects due to their self-amplification through

replication and propagation (Russell et al., 2014). Another beneficial aspect of oncolytic viruses is their ability to target systemic metastases and most notably cancer stem cells which are regarded as being responsible for tumor relapse and chemo-resistance since they are capable of self-renewing after having been treated with cytotoxic drugs (Smith et al., 2014).

Beyond the direct impact on cancer cells, the impact on the tumor environment has to be also recognized. Tumor cells are normally embedded in a very hypoxic and acidic microenvironment, as they are supplied by blood only through leaky and thin-walled blood vessels. Keeping this in mind, oncolytic viruses are capable of inhibiting blood flow to the tumor side, thereby inducing ischemic cell death. The underlying mechanism is not totally understood yet but a reduction in blood vessel density, a destruction of vasculature that cause haemorrhage into tumor tissue as well as virus-induced neutrophils-promoted clot formation have been observed (Bourke et al., 2011, Breitbach et al., 2007, Huszthy et al., 2010, Breitbach et al., 2011).

A big problem in establishing new therapeutic strategies, especially in the treatment of cancer, is based on adverse reactions that even could occur after a long period. In respect thereof, the safety of oncolytic viruses has been proven in over 500 treated patients during the last 20 years of clinical studies. During this time, only one OV-treated patient died due to rapid tumor lysis. Typical side effects are flu like symptoms and in some cases thrombocytopenia and vascular leakage caused by fast intravenous injection (Liu et al., 2007).

Nonetheless, oncolytic viruses are faced with several obstacles on their way conquering cancer. When administered intravenously, viruses are eliminated in the liver, bound by immune cells or inactivated by pre-existing antibodies and complement factors due

to a prior infection or vaccination. As a consequence, OVs are impaired in their effectivity (Breitbach et al., 2007, Chiocca, 2008). In order to circumvent systemic removal, direct injection into the tumor mass has to be considered as an alternative. But since oncolytic viruses should serve as systemic therapeutics with curative intention, both the primary tumor and metastases should be attacked. Therefore, researchers were prompted by the idea to combine oncolytic viruses with supporting drugs in order to enhance oncolytic effectivity. This point will be discussed below.

1.3. Measles virus

1.3.1. Common features

Measles virus (MeV) belongs to the genus Morbilliviruses of the family Paramyxoviridae. Further members are the rinderpest virus (RPV) and the canine distemper virus (CDV).

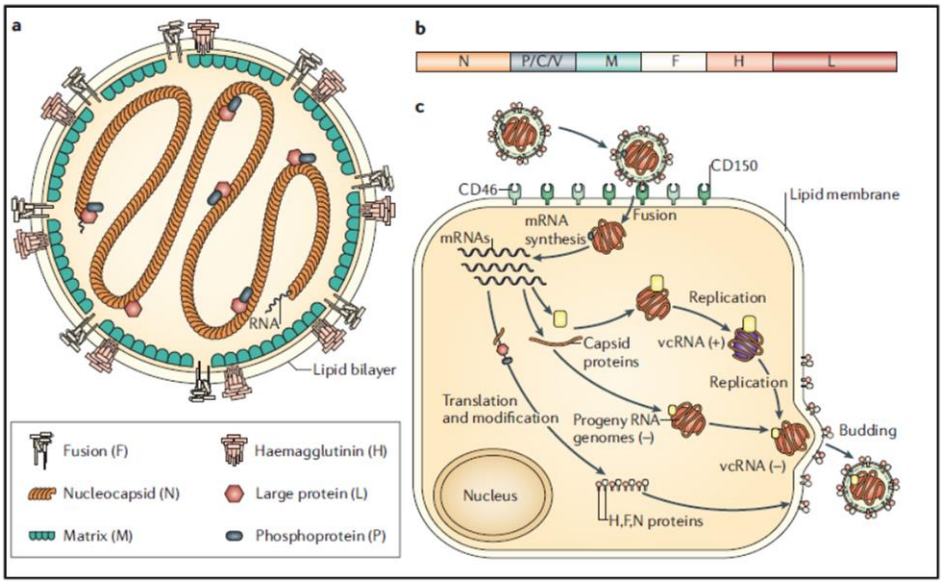

Figure 4: Typical features of measles viruses

a) schematic image of an entire virion; b) structure of measles virus genome; c) representation of a measles virus life cycle. Figure from Moss et al. (Moss and Griffin, 2006)

They are enveloped viruses with a non-segmented, negative-strand RNA genome, containing six different genes. Due to post-translational modifications eight proteins are translated and consequently form the entire virion (Fig. 4): the nucleocapsid (N), phospho- (P), matrix (M), fusion (F), haemagglutinin (H) and large (L) proteins (Yanagi et al., 2006). The F and H proteins are key factors for penetrating host cells. To do so, they interact with CD46, which is expressed on all nucleated human cells, and SLAM (signaling lymphocyte activation molecule), which is only expressed in immune cells, thereby inducing membrane fusion and virus uptake. After viral RNA has been transcribed, the F and H proteins are present on infected cells causing cell to cell fusion and subsequently formation of multinucleated giant cells. The M protein which is located in the inner surface of the envelope is involved in virus budding and transcription regulation. The nucleocapsid consists of the N, L and P proteins, the latter can undergo posttranslational modifications, originating the non-structural C and V proteins (Yanagi et al., 2006, Sato et al., 2012, Msaouel et al., 2012). These proteins were shown to impair the innate immune response by antagonizing type I IFN signaling and additionally enhance autophagic flux in host cells (Richetta et al., 2013).

Regarding measles viruses as human pathogens, they may cause fever, cough and coryza, as well as respiratory and gastrointestinal diseases. In the worst scenario infected people may develop fatal lung and brain complications (Sato et al., 2012, Msaouel et al., 2013).

1.3.2. Measles as an oncolytic virus

The most striking benefit of using measles as an oncolytic agent can be deduced from the experience that has been gained in vaccination programs for many years. In conclusion, safety as well as effectivity could be prosperously proven during the immunization

of over one billion recipients (Lievano et al., 2012, Hutzen B, 2015). Indeed, progenies from the attenuated virus vaccine (Edmonston strain) were found to have the ability to of destroying cancer cells both in vitro and in vivo (Guillerme et al., 2013). Since MeV-Edm serves as a vaccine, it has to be apprehended that the application to almost an entire population is connected with limitations in the administration of measles as oncolytic viruses due to the induced immunity, most prominently represented by neutralizing antibodies. Viruses are a potential source of danger for the population due to their mutability, pathogenicity and transmissibility. However, there has never been a report on a reversion to wild-type measles (Russell and Peng, 2009).

Whereas wild-type measles virus typically infects lymphocytes via SLAM, laboratory derivatives obtained from the Edmonston strain, prefer CD46 for membrane fusion and virus uptake, since they have acquired a relative entry receptor tropism as a result of changing amino acid 481 in the H-attachment protein from asparagine to tyrosine (Nielsen et al., 2001).

CD46 physiologically inactivates complement factors C3b and C4b, thus shielding cells from autologous complement destruction (Msaouel et al., 2013). For this reason, it is supposed that CD46 is frequently overexpressed in cancer cells (Fishelson et al., 2003), leading to the avoidance of cell lysis through complement activation (Guillerme et al., 2013) but therefore making them an easy selective target for MeV. Remarkably, the cytopathic effect (CPE) induced by MeV correlates with the CD46 density on infected cells (Anderson et al., 2004).

The typical pathogenic feature of infected cells is represented by the formation of syncytia carried out by the F and H proteins. Thereby neighboring cells are forced to form multinucleated giant cells, in this way offering measles virus a platform for efficient replication (Guillerme et al., 2013, Takeuchi et al., 2003). Since

even uninfected cancer cells are targeted to form syncytia by infected cells, MeV exhibits a remarkable bystander effect (Msaouel et al., 2012).

Regarding oncolytic selectivity, healthy cells are not affected by the formation of syncytia, since they ordinarily do not exceed a minimal threshold of CD 46 density which is required for virus-induced cell to cell fusion (Anderson et al., 2004, Russell and Peng, 2009).

In summary, MeV is well suited to conquer cancer cells due to its relative selectivity for CD46 receptor, which is expressed with a high density on cancer cells. In addition, the ability of initiating cell to cell fusion, including neighboring uninfected cancer cells offers the additional benefit of inducing a bystander effect (Hutzen B, 2015). Hence, these characteristics delimit and favor them from other OVs and. In this context, another benefit compared to several other virotherapeutics, is their RNA genome. In contrast to DNA viruses such as adenovirus or herpes simplex virus, treatment with MeV is not associated with the possibility of insertional mutagenesis (White et al., 2014).

1.3.3. Genetical engineering of oncolytic measles virus

Measles viruses as many other oncolytic viruses display a well suited vector for introducing genes that enhance their therapeutic effectivity. Those genetic modifications can be grouped due to their effect in those for monitoring, increase in cancer selectivity, arming and immune-modulatory functions (Fig. 5).

In this dissertation, measles virus encoding for green fluorescent protein (GFP) was used (Duprex et al., 1999), since it can be easily visualized by employing fluorescence microscopes (Hutzen B, 2015). In order to obtain a maximal transcription rate of GFP, the gene was inserted into the 3´end of measles genome upstream of the N gene (Duprex and Rima, 2002).

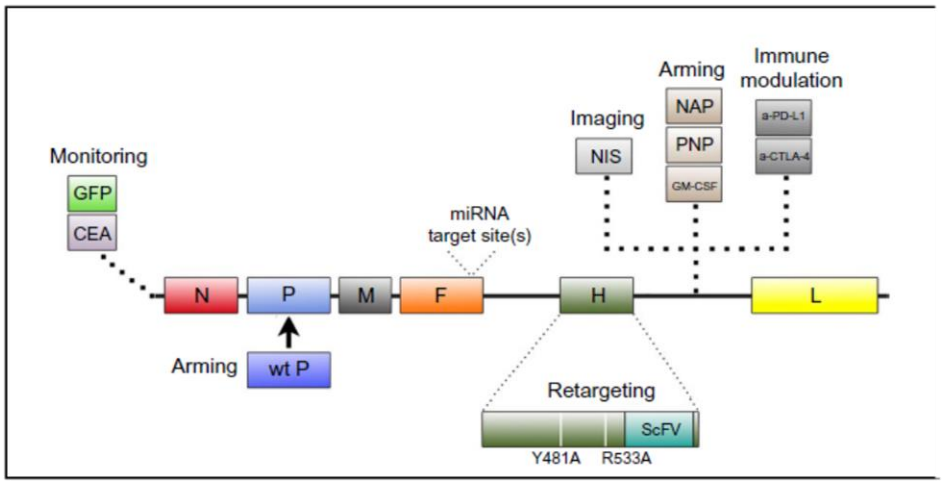

Figure 5: Possibilities for genetically engineering of measles virus genome
Taken from (Hutzen B, 2015)

Considering oncolytic virotherapy of patients suffering from pancreatic cancer, MeV was made selective for pancreatic cancer cells by changing the tropism from CD46 to prostate stem cell antigen (PSCA) which is not expressed on healthy tissue but numerously on pancreatic adenocarcinoma (Bossow et al., 2011).
As stated above, the wild-type P protein impairs the host cell anti-viral immune response. Since the Edm-Strain has lost its P protein-function, MeV was equipped with the wild-type P gene in order to circumvent production of type I IFN by infected tumor cells, thereby facilitating virus replication and spread. Due to concerns of enhanced pathogenicity, no clinical evaluation has been preceded although in vitro experiments as well as animal studies revealed beneficial results (Haralambieva et al., 2007, Hutzen B, 2015).
Following the present trend of exploiting the antitumor immune response in order to contain and delay tumor progression and metastasation in advanced tumor stages, MeV was already endowed with transgenes, encoding for GM-CSF and antibodies against CTLA-4 as well as PD-L1 resulting in encouraging findings (Engeland et al., 2014, Grossardt et al., 2013).

To summarize the possibility of genetically modifying the MeV genome, there is a broad spectrum of approaches which enables a very specific targeting of distinct cancer types in clinical use.

1.3.4. Clinical trials

Several measles strains have been already tested in clinical practice to be safe and efficient. The first clinical trial that investigated a derivate from the Edmonston-Zagreb strain, was conducted in 2005, examining its therapeutic potential in five patients with cutaneous T-Cell Lymphoma (CTCL). Simultaneously, IFN-α was administered in order to avoid systemic complications due to virus infection. Tumor regression could be observed in 60% of treated patients and even more remarkably, distant lesions showed regression (Heinzerling et al., 2005). Since then, more clinical studies were performed and are still ongoing, respectively (Pol et al., 2014). Notably, two patients suffering from Multiple Myeloma, who were pretreated with several established chemotherapeutics as well as immunotherapeutics, a complete durable remission was recently achieved by a single injection of a specific measles virus (MeV-NIS) (Russell et al., 2014).

1.4. Histone deacetylase inhibitors

1.4.1. Histone deacetylases and their physiological function

Cells and even cell nucleuses are only a few µm in diameter but still have to contain the entire human genetic information which is encoded in the DNA. Due to its length of at least two meters, the double-helix has to be condensed to a very small space. Therefore, it is wrapped around specific proteins, called histones. Those display lots of positive charged amino acids (lysine residues), attracting negatively charged DNA and thus forming a very tight formation. The dynamic interplay of acetylation and deacetylation of

lysine residues, as well as further modifications like methylation, ubiqutination and phosphorylation enable a coordinated regulation of gene expression (Abend and Kehat, 2015, Kouzarides, 2007). Mechanistically, deacetylation of lysine residues allows the negatively- charged DNA to bind stronger to histones, thereby compacting chromatin structure, impairing and inhibiting gene transcription (Khan and La Thangue, 2012).

Enzymes being involved in this process are histone deacetylases (HDAC) and histone acyltransferases (HAT) (Abend and Kehat, 2015). Here, we will just focus on HDAC, since they are the target structure of the inhibitor employed in this dissertation. This enzyme family consists of 18 different members which are grouped in four classes due to their sequence homology to Saccharomyces cerevisiae (Abend and Kehat, 2015). Regarding the different classes, class I, II and IV are Zn+-dependent whereas class III inhibitors, also named sirtuins, are NAD+-dependent. In relation to this classification, more precise investigations indicate that each class of HDAC is involved in the execution of specific tasks (Dokmanovic et al., 2007). Class I enzymes are involved in cell survival and proliferation, while class II accomplish tissue specific functions, for instance expression of HIF-α, induction of vascularisation and chondrocyte differentiation. Class IV HDACs (only HDAC 8) are considered to be a combination of class I and II, as they yield typical functional and structural features of both (Dokmanovic et al., 2007).

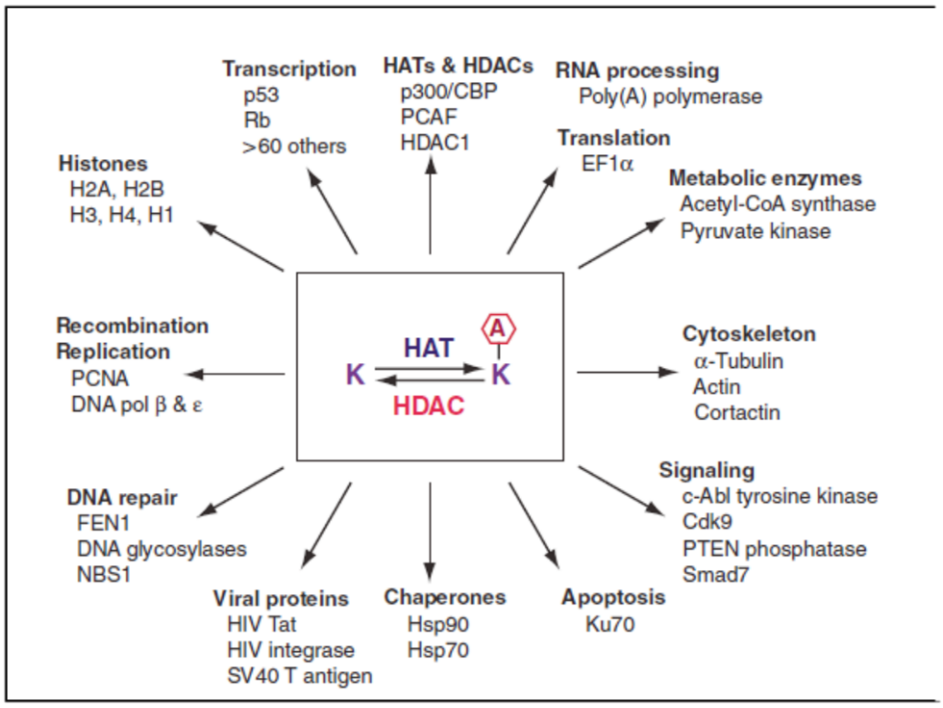

Figure 6: Interplay of HDACi and HATs
Processes which are regulated through acetylation and deacetylation of different lysine residues catalysed by HATs and HDACs (Yang and Seto, 2007)

Considering acetylation as a typical co- and post-translational modification of proteins, almost 85% of all cellular proteins are involved in this process (Polevoda and Sherman, 2000). Due to its unique implementation in cell signaling, several tasks, including enzymatic activity as well as stability, DNA binding, protein-protein interaction and peptide-receptor recognition are executed by this crucial process (Polevoda and Sherman, 2002). But not all acetylating enzymes are suitable targets for HDACi, as they are only capable of deacetylating proteins on ε-amino acids of lysine residues (Glozak et al., 2005). Nonetheless, beyond their ability to deacetylate histones, more and more non-histone proteins have been learned being substrates of HDACs. For this reason the terms lysine deacetylases (KDACs) and protein deacetylases (PDACs) have been established (Rajendran et al., 2011). Important substrates are transcription factors such as NF-κB or p53 as well as STAT proteins which are responsible for mediating signals of

proliferation, survival and immune response (Spange et al., 2009). After having been deacetylated, those proteins either bind stronger to the DNA, thereby enhancing transcription rate, or they forfeit their affinity to DNA with the result of decreasing gene transcription (Park et al., 2015). Additionally, HDAC6 which is localized in the cytoplasm seems to possess an important function in aggresome-formation and may therefore ensure cell viability if cells are exposed to cellular stress induced by misfolded proteins (Kawaguchi et al., 2003).

Since HDACs are essential for an adequate balance between apoptosis and proliferation, several of them were found being overexpressed in different tumor entities (Dokmanovic et al., 2007, Buchwald et al., 2009, Glozak and Seto, 2007). With respect to the topic of this dissertation, an enhanced expression of HDAC 1, 2 and 7 was detected in samples of patients suffering from pancreatic cancer (Fig. 7), supporting tumor maintenance and further progression (Schneider et al., 2010). Presumably, a decreased expression of the cyclin-dependent kinase inhibitor p21 is one of the best investigated changes due to overactivity of HDACs, in this way imitating a loss of function mutation and subsequently preventing the cell from initiating cell cycle arrest (Glozak and Seto, 2007). Another typical feature of epigenetic changes in tumor cells is the hypoacetylation of histone H4, indicating an increased HDAC activity (Fraga et al., 2005).

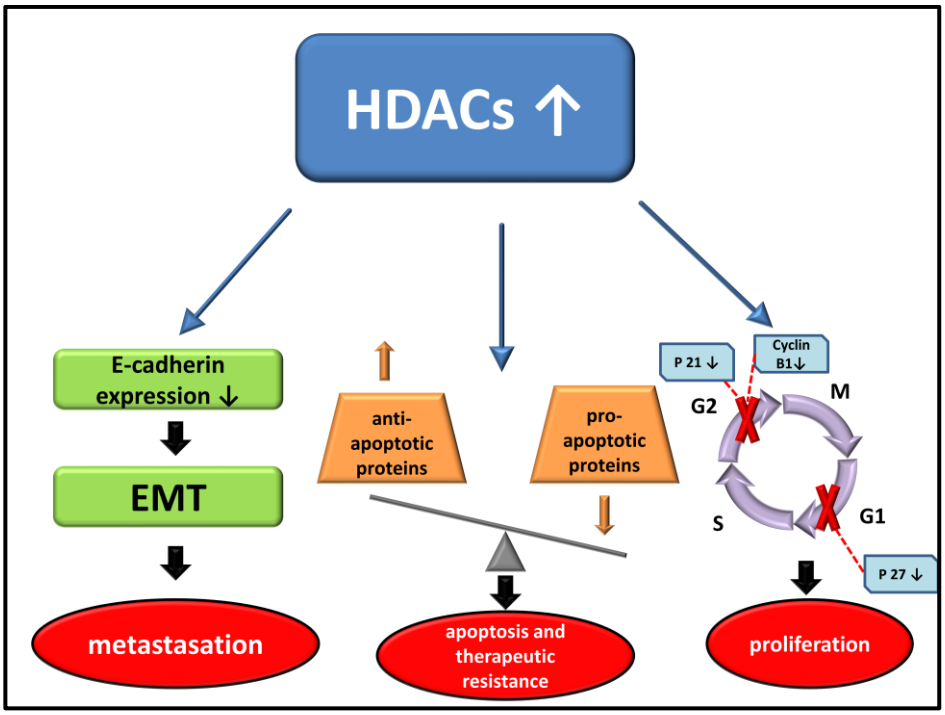

Figure 7: Impact of HDAC overactivity in pancreatic adenocarcioma
Left: impaired expression of E-cadherin facilitates EMT (epithelial-mesechymal transition) and thereby the process of metastasation; middle: HDAC promote an imbalance between anti- and pro-apoptotic proteins, causing apoptosis as well as therapeutic resistance; right: Acceleration of cell cycle, increasing proliferation; figure based on (Schneider et al., 2010)

Taken together, overexpression and / or an enhanced activity of HDACs could be regarded as one major cornerstone for both tumorigenesis and tumor progression and thus display a promising target for anticancer therapy.

1.4.2. Histone deacetylase inhibitors: impact on cancer and immune cells

Back in 1977, Riggs and colleagues already observed that n-Butyrate cause hyperacetylation of histone proteins accompanied by alterations of gene expression (Riggs et al., 1977). The underlying mechanism of inhibiting enzymes endued with the ability of deacetylating proteins was discovered one year later (Sealy and Chalkley, 1978, Boffa et al., 1978).

HDAC inhibitors (HDACi) are solely capable of inhibiting enzymes containing zinc in their catalytic centre, thus not affecting the NAD+-dependent sirtuins (class III HDACs). Because of their different

chemical structure, they are divided into four different groups: hydroxamates, cyclic peptides, aliphatic acids, and benzamides. Another differentiation is based on their selectivity. On the one hand, there are pan-inhibitors including panobinostat, belinostat, trichostatin A, vorinostat and resminostat. One the other hand, there are selective ones like valproate (VPA), inhibiting only class I and IIa HDACs or romedepsin, being class I selective (Khan and La Thangue, 2012).

Their anticancer effect is based on their ability of inducing cell death and preventing further tumor progression by intervening in several different signaling pathways. In this manner, they function as cell cycle inhibitors, cause an accumulation of reactive oxygen species (ROS), induce apoptosis via both the extrinsic and the intrinsic apoptotic pathway and furthermore it is believed that they act like taxanes by impairing mitosis (Khan and La Thangue, 2012). Despite their capability of immediately inducing cell death, they were shown to inhibit tumor angiogenesis by suppressing transcription of HIF-α and VEGF, hence stopping the supply of nutrients and oxygen followed by cell necrosis and / or apoptosis, respectively (Khan and La Thangue, 2012). In addition, they may preclude cells from metastasizing by impairing gene transcription of matrix metalloproteinases (MMP) which are regarded as being involved in intravasation as one of the first steps of metastasation (Bolden et al., 2006, Deryugina and Quigley, 2015). Like oncolytic virotherapeutics, the most striking and valuable benefit of HDACi toward other classical cytotoxic drugs is equally based on their relative tumor selectivity (Bolden et al., 2006).

Beyond their direct effect on cancer cells, HDACi are also relevant due to their impact on the immune system. This effect is carried out in two different ways. On the one hand, HDACi are capable of enhancing MHC-I expression as well as the expression of co-stimulatory / adhesion molecules such as CD40, CD80, CD86 both

on cancer cells and antigen-presenting cells (APCs), thereby facilitating especially cytotoxic T cells the detection and subsequently the elimination of those mutated cells. Helper T cells in turn initiate a powerful systemic anti-tumor-immune response (Bolden et al., 2006, Setiadi et al., 2008). Further important genes were found being HDACi-related upregulated with an emphasis on tumor specific antigens (TAAs) (Kroesen et al., 2014). On the other hand, HDACi both directly and indirectly alter the cytokine secretion of immune cells, affecting most of all type I IFN signaling but also the production of different interleukins and pro-tumorigenic cytokines (Bolden et al., 2006, Kroesen et al., 2014).

Regarding the impact on NK cells as important players in the recognition and eradication of cancer cells, studies have yielded contradictory findings so far (Moretta et al., 2005). It was revealed both an upregulation and a downregulation of ligands on tumor cells as well as NK cells themselves. Although HDACi treatment leads to a positive change in NK cell activation through signals from tumor cells, it was ascertained that their production of cytotoxic proteins like granzyme b and granule release in sum decreases (Ogbomo et al., 2007, Alvarez-Breckenridge et al., 2012, Kroesen et al., 2014). In conclusion, the diverging in vitro results with regard to NK cells do not seem to be transmittable to the impact on an entire living organism and thus, has to be studied in vivo in more detail.

1.4.3. Clinical application of HDACi

Since HDACi had revealed their potential of killing tumor cells efficiently in vitro, they have been investigated in clinical trials, showing promising results, especially in the treatment of hematological malignancies (Mottamal et al., 2015). Therefore, three HDACi were approved by the FDA to date: Vorinostat for the treatment of patients with cutaneous T-Cell Lymphoma (CTCL), romedipsin for application to patients with peripheral T-cell

lymphoma (PTCL) and third, belinostat for treatment of patients with relapsed or refractory PTCL. Beyond their positive effect on neoplasias concerning blood cells, they have already shown encouraging results in the treatment of solid tumors and still more studies are being conducted at the moment (Mottamal et al., 2015). Nonetheless, application in combination with other drugs seems to be even more promising (Thurn et al., 2011). Thus, HDACi have been combined with classical chemotherapeutics, radiotherapy and hormone therapies eliciting synergistic effects regarding both the induction of cell death and the overcoming of drug resistances (Park et al., 2015).

With respect to potentially occurring side effects, hyponatremia, neutropenia, anemia, diarrhea and fatigue were observed in clinical trials so far. Nonetheless, HDACi are altogether well tolerated (Koutsounas et al., 2013, Mottamal et al., 2015).

1.4.4. Resminostat

Similar to vorinostat resminostat is a hydroxamic acid-based HDACi which is an orally administered pan-inhibitor of class I and II HDAC enzymes (Brunetto et al., 2013). It exhibits the typical effects of HDACi. In this manner, treatment with high doses induces potently apoptosis whereas the application of lower doses leads to cell cycle arrest (Mandl-Weber et al., 2010). Concerning the tolerability of resminostat, a phase I study, investigating pharmacokinetics and pharmacodynamics clearly demonstrated that the drug is well tolerated. No other adverse reactions than those which have already been observed after treatment with HDACi in general, have been occurred (Brunetto et al., 2013). To further determine the potential of resminostat, several trials are being performed at the moment investigating the therapeutic effect in patients with advanced stage HCC (NCT00943449), patients suffering from

refractory Hodgkin's lymphoma (NCT01037478), and patients with advanced colorectal cancers (NCT01277406).

1.5. The epi-virotherapeutic approach – state of research

1.5.1. Rationale

As stressed above, oncolytic viruses are faced with different obstacles on their way conquering cancer, particularly, decreases in viral receptor expression (Li et al., 1999, Haviv et al., 2002, Kim et al., 2002), activation of intracellular tumor defense against viral infection (Berchtold et al., 2013, Escobar-Zarate et al., 2013) as well as virus clearance by the host cell immune system (Chiocca, 2008). These observations prompted researchers to look for possible supporting agents. Lots of trials have already investigated the effect of a combination between OV and classical chemotherapeutics (reviewed in (Fillat et al., 2014)). In this way, several different combination settings could reveal promising effects, especially emphasizing that there are no cross-resistances between OV and chemotherapeutics (Cripe et al., 2009). But due to potentially occurring severe adverse effects, cytotoxic agents should be preferably replaced by drugs that are better tolerable.

Implementing the epi-virotherapeutic approach, represented by a combination between HDACi and OV, encouraging results have been achieved both in vitro and in vivo. The underlying mechanisms could be partly elucidated revealing several synergistic working points while being relatively selective to tumor tissue (MacTavish et al., 2010, Nguyen et al., 2010, Ruf et al., 2015) (Fig. 8).

“

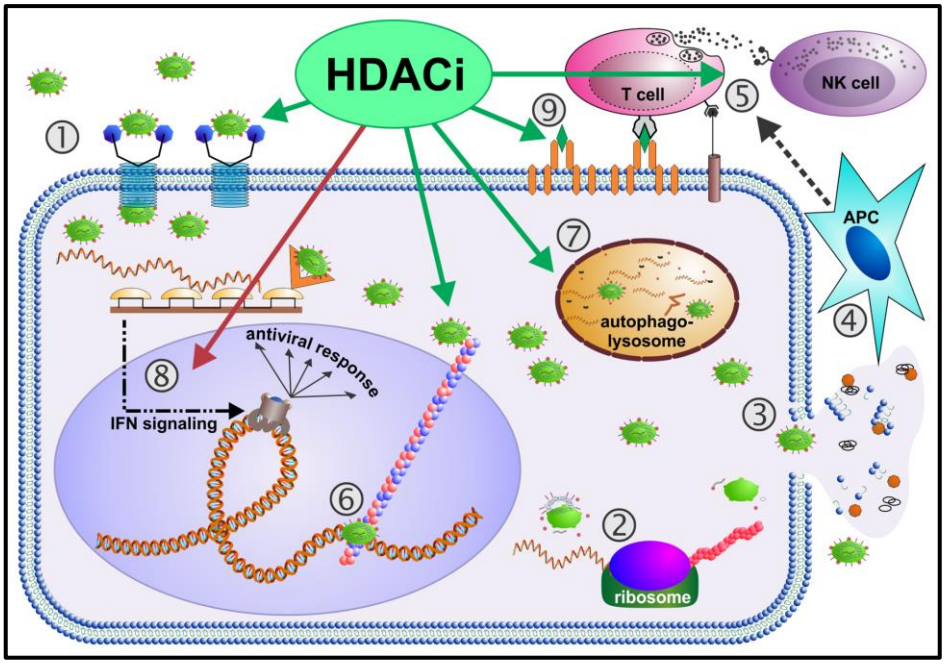

Figure 8: Virus-induced oncolysis augmented by histone deacetylase inhibitors (HDACi)
Following receptor binding (1), oncolytic viruses OVs infect tumor cells. Then, host cell ribosomes are occupied with translation of viral RNA into viral structural/functional proteins (2), resulting in generation of numerous progeny viral particles per single host tumor cell. This enormous replicative process ends up in complete exhaustion of host tumor cells, inescapably leading to tumor cell disintegration, i.e., viral oncolysis. Thereby, not only newly produced viral particles are released (3), but also tumor-associated antigens (TAAs) and damage-associated molecular pattern molecules (DAMPs), which are detected by antigen-presenting cells (APCs) (4) (Kaufman et al., 2015). Concurrently, OV infection induces production of pro-inflammatory, immune cell-attracting cytokines, which also exert potent antitumor activities (Prestwich et al., 2009). Furthermore, OV infections upregulate MHC-I expression on tumor cells (Gujar et al., 2013). Altogether, APC activation, production of antitumor cytokines and upregulation of antigen-presenting receptors are assumed to initiate a powerful T cell-mediated antitumor immune response (5) (Moehler et al., 2005, Kaufman et al., 2015). Notably, all these steps of the viral oncolytic cycle (1-5) can be influenced by histone deacetylase inhibitors (HDACi): first of all, HDACi can upregulate expression of viral entry receptors on tumor cells leading to increased rates of tumor cell infection by OVs (1) (Wunder et al., 2013, Kasman et al., 2012, Nguyen et al., 2010). Further, translocation of OV genomes, i.e., post-entry shuttling to the nucleus via microtubules (6) can be increased by HDACi (Nakashima et al., 2015a). Next, expression of viral genes can be augmented by HDACi in tumor cells (Nakashima et al., 2015b, Otsuki et al., 2008, Nakashima et al., 2015a). HDACi-enhanced tumor cell autophagy (7) can result in increased OV-mediated oncolysis and enhanced induction of tumor cell apoptosis (Shulak et al., 2014). Remarkably, HDACi were also found to be able to dampen antiviral IFN responses being characteristic for OV-resistant tumor cells (8) (Berchtold et al., 2013, Escobar-Zarate et al., 2013), thereby significantly facilitating OV replication and spread (Nguyen et al., 2010, Ruf et al., 2015, Otsuki et al., 2008, Nguyen et al., 2008). In terms of boosting immune cell-mediated antitumor response, HDACi can raise the levels of cytokines being supportive for the functional development of tumor antigen-specific CD8+ T cells (5) (Bridle et al., 2013). Beyond that, HDACi can also inhibit T- and NK cell-mediated antiviral responses, supporting an unimpaired OV replication and propagation in tumor cells (Bridle et al., 2013, Alvarez-Breckenridge et al., 2012). As HDACi can also cause upregulation of MHC-I molecules, co stimulatory receptors as well as TAAs (9) (Bolden et al., 2006, Kroesen et al., 2014, Setiadi et al., 2008), it is tempting to speculate that combined epi(HDACi)-virotherapeutic approaches might further amplify the magnitude of antitumor immune response. Taken together, OV-induced oncolysis can be

augmented by HDACi in many steps and on numerous levels of the interaction between host tumor cells and OVs." (Ellerhoff et al., 2016)

1.5.2. Overview over synergistic working points

Although most cancer cells exhibit defects in their antiviral immune response, there are still cancer cells, being equipped with an intact or even reinforced response to invaders, most commonly due to mutations in the IFN-pathway (Escobar-Zarate et al., 2013, Stojdl et al., 2003). For instance, an enhanced expression of retinoic acid inducible gene I (RIG-I) and interferon-induced protein with tetratricopeptide repeats 1 (IFIT1) could be attributed to a resistance of different sarcoma cell lines against MeV-SCD (Berchtold et al., 2013). Both represent antiviral effector proteins which detect and subsequently initiate the elimination of invaded viruses and their expression is induced by IFN-signaling in order to detect and eliminate viruses (Schoggins and Rice, 2011).

Since HDAC interact with enhancers of IFN-genes and are moreover involved in the expression of interferon-stimulated-genes (ISGs) (Nusinzon and Horvath, 2006, Kadota and Nagata, 2011), HDACi are indeed capable of damping the host cell IFN-response, thereby enhancing virus-mediated replication and spread through tumor tissue (Vlasakova et al., 2007) (Fig. 8). Remarkably, cells which had been primarily resistant toward OVs could be made susceptible due to HDACi treatment (Nguyen et al., 2008, MacTavish et al., 2010).

Autophagy is a catabolic process which describes the degradation of cellular components and recycling in lysosomes in order to maintain a cellular homeostasis. Furthermore it serves as a response to stress, lack of nutrients, hypoxia, as well as for the elimination of intracellular pathogens like bacteria and viruses (Murrow and Debnath, 2013). Several studies revealed that some viruses profit from the pharmacological induction of this pathway, thereby enhancing their anticancer activity (Meng et al., 2013). In

this context, vorinostat in combination with vesicular stomatitis virus (VSV) led to an enhanced oncolytic effect via an upregulation of autophagy stimulated genes (ATG101, ATG7, and GABARAPL1) (Shulak et al., 2014).

As another important synergistic working point, an enhanced expression of virus entry receptors could be observed due to HDACi treatment (Fig. 8). This mainly applies to coxsackie- and adenovirus receptor (CAR) which was found being frequently downregulated in several different tumor entities (Saito et al., 2014). The molecular mechanism, causing this phenomenon, was shown to be of epigenetic origin and thus, is in posse to be modified by treatment with HDACis (Sachs et al., 2004, Ma et al., 2012). There is further evidence that entry receptors of other viruses can be upregulated as well. A conjunction treatment of an equine HSV (EHV) and VPA in human glioblastoma cells resulted in an increased virus entry when VPA was given 24 hours before virus infection. In the same manner, an enhanced viral spread was observed. The authors suggest that these findings could be explained by MHC-I upregulation which can serve as an entry receptor for EHV, since it is capable of binding to the glycoprotein D (White and Frampton, 2013).

Considering the application in vivo, both agents have proven their positive impact on the immune system. Because of these findings, one might suggest that the combination is able to elicit even more remarkable effects. In order to prove this thesis, clinical studies have to be conducted but are still outstanding. However, in an integrated approach investigating a combination of a viral vaccine, an OV and a HDACi (entinostat), the secondary antitumor immune response was not further enhanced following HDACi application but fortunately, a lower production of neutralizing antibodies as well as decreased numbers of T cells, directed against the OV, were observed (Bridle et al., 2013).

1.6. Objectives

Based on an auspicious preliminary study conducted by our research group, investigating a combination of oncolytic measles virus armed with a prodrug convertase (MeV-SCD) and the HDACi resminostat on different hepatoma cell lines (Ruf et al., 2015), the aim of this dissertation was to evaluate this specific epi-virotherapeutic approach for the treatment of advanced pancreatic cancer and to gain further inside into a possible synergistic mode of action. Regarding synergistic working points found in our previous work, it was pointed out that resminostat hindered tumor cells to express ISG in hepatoma cell lines (Ruf et al., 2015). Furthermore, an induction of apoptosis was observed and even more strikingly, no impairment of virus replication and propagation could be revealed.

Since pancreatic cancer is associated with a miserable prognosis and there is still a dramatic lack in efficient therapeutic options, it should be regarded as a tumor entity that is well suited for establishing new therapeutic agents. In respect thereof, our previous results from the treatment of HCC should be tested for a broader spectrum of efficiency, i.e. in pancreatic cancer as well.

2. Materials and Methods

2.1. Safety of laboratory

All experiments described below were performed in our laboratory at the Hertie-Institut, Tübingen, complying Biosafety Level 2 of the Directive 2000/54/EC, biological agents at work from the European Parliament from the year 2000. In order to accomplish these requirements, most of the work was executed under a laminar flow hood (HERAsafe). Before and after usage the work surface was cleaned with 70% Isopropanol (SAV Liquid Production; Flintsbach a. Inn, Germany) or Descosept (Dr. Schuhmacher GmbH; Melsungen, Germany) in case of experiments involving oncolytic viruses, respectively. After use, all materials were additionally irradiated with UV-light to inactivate viral particles and then autoclaved.

2.2. Pancreatic cancer cell culture

Pancreatic cancer cell lines (AsPC-1, BxPC-3, MiaPaCa-2 and PanC-1) obtained from the European Collection of Authenticated Cell Cultures (ECACC) were cultured in cell culture flasks in Dulbecco's modified Eagle's Medium (DMEM) (SIGMA high glucose; 4.5 g/L; L-Glutamine) containing 10% fetal calf serum (FCS) (DMEM-10). To provide optimal living conditions, cells were kept under humid atmosphere in an incubator at 37°C containing 5% CO_2. Sterile working conditions were ensured by the work bench HERAsafe.

2.2.1. Harvesting and splitting of cells

Cell cultures were passaged about twice a week in order to avoid a lack of nutrients and a deceleration of cell division rate.

Initially, the old medium had to be aspirated, afterwards cells were gently washed with pre-warmed (37°C) phosphate buffered saline (PBS). To detach cells from the flask bottom, EDTA-trypsin was added and cells were incubated at 37°C till they were disengaged

from the bottom (duration differed between different cell lines). Then fresh DMEM-10 was added to inactivate trypsin. 1/2 to 1/10 of the cell suspension was kept for further cultivation. Flasks were refilled with fresh medium and placed in the incubator again.

2.2.2. Cryoconservation of cells

To provide a continuous supply of fresh cells, five cryovials of pancreatic cancer cells from each cell line were frozen at -180°C. For this purpose, cells were trypsinized as described above and the cell suspension was centrifuged at 1200 rpm for five minutes at room temperature. The cell pellet was resuspended in DMEM containing 10% dimethylsulfoxide (DMSO) and 20% FCS. 1 ml aliquots were transferred into cryovials and frozen at -80 °C. The next day they were transferred to -180 °C.

2.2.3. Thawing of cells

When new cells had to be taken into culture, cryovials were removed from the freezer and thawed quickly at 37°C in the water bath. Then cells were diluted in fresh pre-warmed DMEM-10 and centrifuged at 1200 rpm for five minutes. The cell pellet was again resuspended in medium and transferred to culture flasks.

2.2.4. Counting cells

Comparable to counting blood cells by employing a microscope, an improved Neubauer haemocytometer was utilized for determining cancer cell concentrations. A Neubauer haemocytometer consists of engraved squares of different size. The large squares at the corners are usually used for white blood cells whereas the subdivided smaller squares in the middle are usually used for red blood cells and platelets. Because of similar size and concentrations of cancer and white blood cells, the four big edge-squares, covering 1 mm^2 were used to count cancer cells.

To exclude dead cells, one tenth of cell suspension was mingled with nine tenths of trypan blue. This aqueous solution was pipetted under the cover glass which had been placed over the counting chamber, leaving a space of 0.1 mm. Since one square covers 1 mm^2 and the distance between the chamber and the cover glass is 0.1 mm, 0.1 µl solution fits into the space, implying that the amount of counted cells had to be multiplied by 10^4. Considering ancillarily the dilution factor of 10, the concentration of cells per ml is given by 10^5 times the counted cells.

2.3. Virological methods

2.3.1. Virus infection of pancreatic cancer cells

Pancreatic cancer cells were seeded in 6-well or 24-well plates the day before treatment (Tab. 1). Measles virus (MeV) was thawed and vigorously vortexed in order to equally distribute the viruses.

Table 1: Summarization of the amount of pancreatic cancer cells per well on 6- and 24- well plates

Pancreatic cancer cell line	6-well plates	24-well plates
AsPC-1	4 X 10^5	4 X 10^4
BxPC-3	4 X 10^5	4 X 10^4
MIA PaCa-2	2 X 10^5	2 X 10^4
PANC-1	2.5 X 10^5	3 X 10^4

According to the required multiplicity of infection (MOI), the amount of applied virus was calculated and diluted in Opti-MEM (Gibco; Grand Island, NY). Old medium was removed from pancreatic cancer cells, cells were washed with PBS and subsequently infected by adding 250 µl of virus dilution. After the infection period of three hours, the inoculum was removed and fresh DMEM-10 was added (Fig. 9). In case of a combination experiment or a mono-

treatment experiment with resminostat (4-SC, Planegg-Martinsried, Germany), the new DMEM medium contained the required concentration of resminostat.

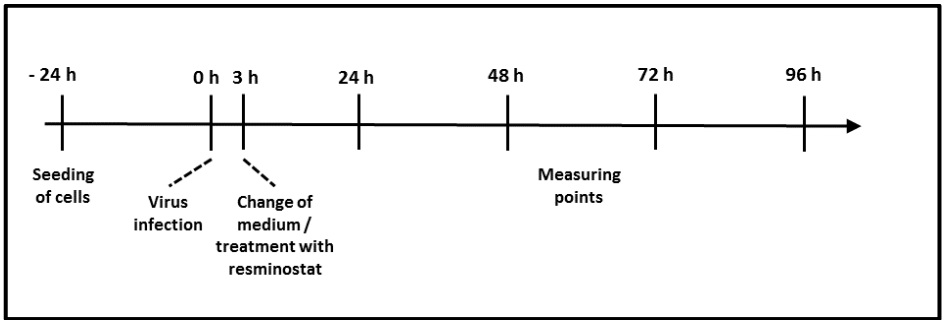

Figure 9: Timeline of virus infection and treatment

2.4. Determining cytotoxicity to pancreatic cancer cells

2.4.1. SRB cell viability assays

The sulforhodamine B (SRB) assay is a very well suited method to perform cytotoxicity screenings. Since the dye binds to basic amino-acid residues of cellular proteins and each cell from one distinct cell line has an almost equal protein composition, it might be assumed that SRB absorption is proportional to the cell mass per well (Vichai and Kirtikara, 2006).

For this reason SRB staining was chosen in order to investigate how many cells in relation to MOCK-treated cells survived virus-mediated oncolysis and HDACi-induced cytotoxicity, respectively. Therefore, medium was removed after the required time period, wells were thoroughly washed with PBS, followed by cell fixation with 10% trichloroacetic acid (TCA). Afterwards, plates were stored for 30 minutes at 4°C and then washed with tap water for four times and stored at 40°C over night until they were entirely dry.

The next day, fixed cells were covered for at least 10 minutes with 250 µl SRB staining solution (0.4% w/v in 1% acetic acid) and afterwards washed with 1% acetic acid. After having been dried

again, one to two ml 10 mM TRIS base solution (pH 10.5) were added to the plates in order to solubilize SRB from cell proteins. Subsequently, 80 µl of the solution from one well were transferred in duplicates to a 96-well plate and the extinction was measured by using a microplate photometer (Tecan Genios Plus) at a wavelength of 550 nm. The results were expressed as percentage of MOCK-treated cells.

2.4.2. Real-time cell proliferation assay

The real-time cell proliferation assay was performed with the xCELLigence system employed (Roche Applied Science, Mannheim, Germany) which is based on electronic impedance sensors integrated on a typical 96-well plate. Since cells adhere to the bottom of wells, the amount of cells and the extent of adhesion are responsible for the electrical impedance. Consequently, an increase in impedance results from a higher amount of cells or an increase in cell adhesion. Measurements were expressed in cell index (CI) value which was determined through the proportion to the initial value. Thus, changes in cell morphology, viability or adhesion induce changes in cell index value (ACEA Biosciences, 2013).

In contrast to other experiments that comprised virus infection and resminostat treatment, no change of medium was performed. Hence, the treatment scheme differed from those of previous experiments (Fig. 10).

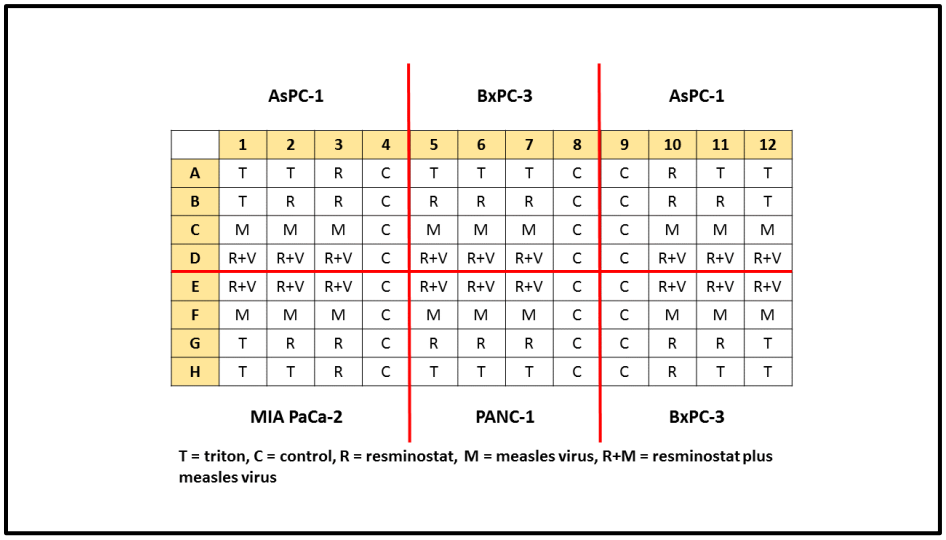

	1	2	3	4	5	6	7	8	9	10	11	12
A	T	T	R	C	T	T	T	C	C	R	T	T
B	T	R	R	C	R	R	R	C	C	R	R	T
C	M	M	M	C	M	M	M	C	C	M	M	M
D	R+V	R+V	R+V	C	R+V	R+V	R+V	C	C	R+V	R+V	R+V
E	R+V	R+V	R+V	C	R+V	R+V	R+V	C	C	R+V	R+V	R+V
F	M	M	M	C	M	M	M	C	C	M	M	M
G	T	R	R	C	R	R	R	C	C	R	R	T
H	T	T	R	C	T	T	T	C	C	R	T	T

Figure 10: Exemplary pipetting scheme of the 96-well plate for xCELLigence

At the beginning the background impedance had to be determined. Therefore, each well was filled with 50 µl DMEM-10 and put in the xCELLigence station at 37°C. Cells were seeded in concentrations with respect to their particular proliferation characteristics which were determined before (AsPC-1:10,000 cells per well; BxPC-3: 2,500 cells per well; MIA PaCa-2: 7,500 cells per well; PANC-1: 5,000 cells per well).

Cells were added in 100 µl DMEM supplemented with only 2.5% FCS. 21 hours after cell seeding, MeV diluted in 10 µl Opti-MEM was pipetted to required wells, infecting at MOIs as commonly used (5 for AsPC-1, 0.5 for BxPC-3, 2.5 for MIA PaCa-2 and 0.25 for PANC-1). Wells that were only MOCK- or HDACi-treated, were equally filled with 10 µl Opti-MEM. Hence, each well contained now 160 µl medium. After three more hours, 50 µl DMEM containing 27% FCS and, if required, additionally resminostat (1 µM for AsPC-1 and MIA PaCa-2, 2.5 µM for BxPC-3 and 5 µM for PANC-1), were added with the result that cell medium was finally supplemented with 10% FCS.

Figure 11: Timeline of combination treatment for xCELLigence experiments

The array of cell lines and mode of treatment were arranged as shown in (Fig. 11).

2.5. Virus growth curves in pancreatic cancer cells

2.5.1. Obtaining virus samples

The four pancreatic cancer cell lines were seeded one day before virus infection in 24-well plates in 500 µl DMEM-10 (Tab. 1 shows the amounts of cells per well for each pancreatic cancer cell line). Measles virus was added in Opti-MEM at MOIs of 0.25, 0.5, 2.5 and 5 for PANC-1, BxPC-3, MIA PaCa-2 and AsPC-1, respectively. Cells were infected as described above. After three hours, Opti-MEM was removed and cells were washed with PBS for three times. Afterwards, 500 µl DMEM-10 were added if required, containing supplementary resminostat in following concentrations: 1 µM for AsPC-1 and MIA PaCa-2, 2.5 µM for BxPC-3 and 5 µM for PANC-1. In order to quantify virus replication over the post infection period, samples were taken at 3, 24, 48, 72 and 96 hours post infection (hpi). Therefore supernatants were transferred into 2 ml eppendorf-tubes, 500 µl Opti-MEM were added to the remaining cells which were finally scraped off the bottom of wells by using a 1000 µl pipette. Cell suspensions were also transferred into 2 ml eppendorf-tubes. Altogether, there were four samples for each time point, in each case two samples with supernatant and two with cell suspension. Both had been treated with measles virus but one of them had been additionally treated with resminostat. All samples

were stored at - 80°C in order to lyse cells and consequently release virus.

2.5.2. Virus titration on Vero cells

Virus growth kinetics were determined by infecting Vero cells obtained from the German Collection of Microorganisms and Cell Cultures (DSMZ, Braunschweig, Germany). In order to quantify viruses, dilution series of samples taken at different points in time, as described above, were prepared. For this purpose, samples were thawed, carefully vortexed and subsequently centrifuged for two minutes at 3000 rpm. 300 µl of each sample were pipetted into a 96-well dilution plate as shown in (Fig. 12).

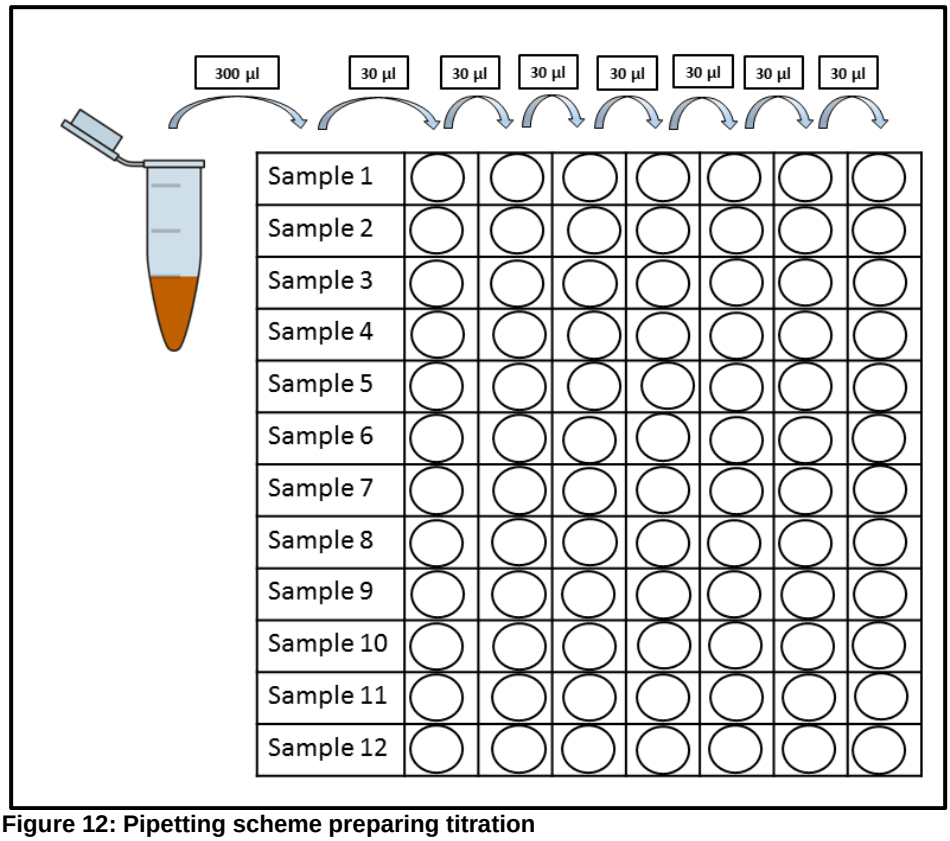

Figure 12: Pipetting scheme preparing titration

All other wells were filled with 270 µl DMEM medium containing 5% FCS (DMEM-5). Finally, 30 µl from the first column were transferred to the next one and resuspended. This step was repeated till the

last column was reached. Consequently, each column contained one tenth of unknown virus concentration as compared to the one before.

After having created this 1:10 dilution series, samples were added to the Vero cells which had been seeded in 96-well plates at a density of 10^4 cells per well in DMEM-5 the day before. Each row of the dilution was used to infect four rows of Vero cells. In order to determine the exact virus concentration, Vero cells were examined whether they were infected with MeV after 96 hours. Since MeV carried a gene encoding for green fluorescent protein (GFP), infected cells produced GFP and consequently, virus infection could be detected and quantified by using a fluorescence microscope. A "positive" well was defined as at least one green plaque, representing a Vero cell syncytium formed due to infection by replication-competent MeV. More precisely, exact concentrations were calculated from the Tissue Culture Infective Dose ($TCID_{50}$) was as described by Spearman and Kärber (Karber, 1931, Spearman, 1908) (Fig. 13)

$$\mathrm{TCID}_{50}\ \frac{1}{\mathrm{ml}} = \frac{N_{\text{viral particles}}}{1\ \mathrm{ml}} = \frac{10^{1+(N_{\text{infected wells}} - 0.5 \cdot \log(10))}}{0.03\ \cdot V_{\text{inserted viral solution}}}$$

Figure 13: $TCID_{50}$-formula by Spearman (1908) and Kärber (1931)

The $TCID_{50}$ is defined as the required amount of virus that is needed to produce a cytopathic effect in 50% of inoculated tissue culture cells.

2.6. Verification of decrease in levels of zinc-finger protein 64

2.6.1. Obtaining RNA samples

Pancreatic cancer cells were seeded in 6-well plates and 24 hours later MOCK-treated, treated with resminostat or / and infected with

MeV-GFP, respectively, applying concentrations and MOIs according to (Tab. 1). After 5 and 24 hours, medium was removed; cells were washed with PBS (2 ml) and afterwards scraped off the bottom of wells in PBS. Subsequently, the cell solution was transferred to a 2- ml Eppendorf-Cup and centrifugated at 5000 rpm for five minutes. In order to isolate RNA from the cell suspension, the NucleoSpin® RNA kit (Macherey-Nagel, Düren, Germany) was employed following the manufacturer´s instructions.

2.6.2. qPCR of zfp 64 mRNA

"RT buffer (Promega, Madison, WI, USA), 1 µl RNase- RNasin Plus (Promega), 1 µl oligo-dT-Primer (0.5 µg/µl) (TIB MolBio, Berlin, Germany), 0.5 µl dNTP mix (Roti-Mix PCR3, Carl Roth) and added up to a total volume of 9.6 µl in RNAse-free water. Samples were then incubated at 70˚C for 2 min. After adding 0.4 µl reverse-transcriptase M-MLV RT H(-) Point Mutant (Promega), samples were incubated at 42˚C for 60 min.

The cDNA samples diluted (1/40) with tRNA-H2O; primers were used in a concentration of 500 nM. PCR was carried out in an iCycler (Bio-Rad) with iQ5 Multicolor Real‑time Detection system (Bio-Rad), using the following setup: 10 µl iQSYBR Green PCR Master Mix (Promega), 0.1 µl of each primer (100 µM stock), 5.8 µl H_2O and 4 µl cDNA (diluted 1/40). The following primer pairs were used: zfp64 (splicing variants 1,3,4) forward, ACCTGCCCACGGAA AGTAAT; zfp64 (splicing variants 1,3,4) reverse, TATGGGG TTTGTCTCCCGTG; RPS18 (housekeeping gene) forward, GAGGATGAGGTGGAACGTGT; RPS18 reverse, TCTTCAG TCGCTCCAGGTCT. PCR was carried out with the following thermal profile: 3 min at 95˚C with subsequently 40 cycles for 15 sec at 95˚C, 20 sec at 58˚C, and 15 sec at 62˚C. Heating up for 1 min at 95˚C was followed by 1 min at 65˚C and 81 cycles at 65˚C cooling down to 20˚C. Target gene expression was evaluated via

the 2-ΔCt method and normalized to the housekeeping gene RPS18 and subsequently graphed relative to the respective mock sample for each time-point and expressed as 'relative gene expression'." (Ellerhoff et al., 2016)

2.7. Detection of IFN-stimulated genes proteins by immunoblotting

2.7.1. Preparation of cell lysates

Pancreatic cancer cells were seeded in 6-well plates (for amounts per well see Tab. 1) and infected with MeV-GFP in presence or absence of resminostat. Furthermore, few cells were stimulated with IFN-β after three hours. After different time periods cells were harvested. For this purpose, medium was removed, cells were washed with PBS and scraped off the wells´ bottom in PBS. Cell suspensions were centrifuged at 4000 rpm for five minutes. Cell pellets were resuspended in lysis buffer (50 mM Tris pH 7.6, 150 mM NaCl, 1% IGEPAL Sigma Aldrich) whereby the required amount depended on the size of the pellet. Cell lysis was performed by three freeze-thaw cycles. Therefore, cell samples were defrosted at 37°C in the water bath and subsequently shock frozen in liquid nitrogen. Finally cells were spun down for ten minutes at 13000 rpm at 4°C and supernatants containing released cellular proteins were transferred to Eppendorf-tubes and stored at - 20°C.

2.7.2. Determination of protein concentration following the Bradford-method

After cell lysis, protein concentrations were determined applying the Bradford method (Bradford, 1976). Therefore, cell lysates were diluted 1:40 with double-distilled water (ddH_2O). According to figure 14, a series of standard dilutions of bovine serum albumin (BSA) covering protein concentrations from 0.5 to 0.05 mg/ml were pipetted in the first two rows of a 96-well plate. To determine the blank value, ddH_2O was added to the dilution row. The remaining

samples were transferred in duplicates to two wells. All wells were filled with 10 µl solution (BSA and cell lysate, respectively) (Fig. 14).

	1	2	3	4	5	6	7	8	9	10	11	12
A	BSA 0.5	BSA 0.25	BSA 0.1	BSA 0.05	dd H_2O							
B	BSA 0.5	BSA 0.25	BSA 0.1	BSA 0.05	dd H_2O							
C	lysate 1	lysate 2	lysate 3	...								
D	lysate 1	lysate 2	lysate 3									
E												
D												
G												
F												

Figure 14: Pipetting scheme for Bradford protein determination

Afterwards, the Bradford reagent (BIO-Rad) was diluted 1:5 with water and 200 µl of this dilution were subsequently transferred to each well. Its component Coomassie Brilliant Blue G-250 dye forms complexes with proteins which shift the absorption maximum from 465 nm to 595 nm. This implies that the higher the concentration of proteins in solution, the greater is the extent of absorption at 595 nm. Therefore, the extinction was measured at 595 nm utilizing the ELISA reader. The precise amount of protein in each sample was calculated on basis of the standard curve of BSA.

2.7.3. SDS-Page

For the purpose of separating proteins according to their size, a sodium dodecyl sulfate polyacrylamide gel electrophoresis (SDS-Page) was performed. This method was initially implemented by

Laemmli (Laemmli, 1970) and takes advantage of the ability of SDS to overlap charges of proteins by disrupting non-covalent bonds. Consequently, polypeptide chains are unfolded and proteins are charged negative. Therefore, they can be separated by size, without considering their charge.

Two gels were prepared applying the formulas shown in (Tab. 2). To bring the gels into shape, two plane parallel glass plates were assembled in a distance of 1.5 mm. Initially, the resolving gel was funneled into the created chamber and then, isopropanol was added to create a flat surface. Since tetramethylethylenediamine (TEMED) serves as a catalyst and ammonium persulfate (APS) as a radical initiator, polymerization starts subsequently after admixture of these two ingredients and took at least 15 minutes. After having discarded isopropanol and washed the gels´ surface with water, the stacking gel was filled over the resolving gel and a comb was inserted to form pockets for protein samples.

Table 2: Ingredients of gels used for electrophoresis

8 % resolving gel (for two gels)	5 % stacking gel (for two gels)
- 9.3 ml ddH_2O - 5.0 ml 1.5 M Tris-HCl pH = 8.8 - 5.3 ml Acrylamide mix 30% - 200 µl 10% SDS - 200 µl 10% Ammonium persulphate (APS) - 12 µl TEMED	- 4.1 ml ddH_2O - 1.0 ml 1.0 M Tris-HCl pH = 6.8 - 750 µl Acrylamid mix 30% - 60 µl 10% SDS - 60 µl 10% Ammonium persulphate (APS) - 6 µl TEMED

vAfter both gels had polymerized, they were put into an electrophoresis chamber which was filled with running buffer (5X buffer: 15.1 g Tris, 72 g glycine, 5 g SDS in 1 l of ddH_2O).

70 µg of each protein sample were enriched with one sixth loading buffer (β-mercaptoethanol) and denaturated in a heating block for five minutes at 95°C. Both steps are essential for breaking down secondary and tertiary structures of proteins, enabling to bring the proteins into the gel pockets. Furthermore, a positive control (IFN-treated) and a molecular weight marker (PageRuler Plus protein ladder (Thermo Scientific, Waltham, MA)) were added to each row of protein samples. The fractionation of proteins was performed by applying a voltage of 70 V and a current of 40 mA, respectively.

2.7.4. Western Blot

With the objective of detecting specific proteins, separated proteins from the cell lysates were transferred from the gel to a polyvinylidene difluoride- (PVDF) membrane (Amersham Hybond P, GE Healthcare). For this purpose, the PVDF membrane and the gels were fastened in spatial proximity by using clamps (sandwich) and were finally put in transfer buffer (Tris 48 mM, Glycine 39 mM, MeOH 20%) applying a current of 300 mA for one hour. After having performed the transfer, membranes were washed with methanol

and stained with Ponceau S red dye solution (Roth; 0.1% (w/v)) to check whether the proteins were actually and accurately transferred to the membranes without air bubbles. Membranes were subsequently blocked for one hour with TBS-T (NaCl 150 mM, Tris 50 mM, adjusted pH (7.4) with HCl, 0.02% Tween) supplemented with 5% milk powder, thereby preventing non-specific binding of antibodies used later. Overnight , membranes were incubated with primary antibodies (anti-IFIT1: GTX103452; 1:1000; GeneTex, Irvine, CA; anti-Phospho-Stat1: 58D61; 1:1000; Cell Signaling Technology, Danvers, MA; anti-Stat1: sc-591; 1:500; Santa Cruz Biotechnology, Santa Cruz, CA; anti-β-Actin: A 4700; 1:6000; Sigma Aldrich) continually pivoted on a shaker at 4°C. The next day, antibodies were removed and membranes were washed with TBS-T three times for ten minutes. Afterwards, membranes were exposed to the secondary antibody (goat anti-rabbit IgG; goat anti-mouse IgG; HRP-coupled; Abcam Ltd., Cambridgeshire, UK) dissolved in 5% milk powder in TBS-T for at least one hour. Then, membranes were washed again three times with TBS-T for ten minutes.

To detect the sought proteins, ECL Western Blotting Detection Reagent (mixed 1:1, GE Healthcare) and photosensitive films (GE Healthcare) were utilized. Therefore, both components of the chemiluminescence kit were mixed in equal amounts and incubated with the membranes for one minute. Afterwards, membranes were covered by plastic sheets and put into photo cassettes (Dr. GOOS Suprema GmbH). Subsequently, films were developed in a dark room. The exposition times varied between different antibodies and protein samples.

After protein bands had been detected, antibodies were stripped off membranes. Therefore PVDF membranes were incubated in 10 mM NaOH for ten minutes and afterwards washed with TBS-T for three times.

Membranes were then reprobed with different antibodies in order to detect further proteins (in this case β-actin and STAT-1).

2.8. Statistical analysis

"The influence of measles and resminostat on the decadic logarithm of cell mass (in % of the mean of the cell line control) was examined by performing a two-way analysis of variance (ANOVA). Additionally, an interaction of measles and resminostat was used in the ANOVA. Calculations were done by the JMP software for windows. P-values <0.01 were considered to be statistically significant. Graphs including error bars were imaged with GraphPad Prism 4 for windows. " (Ellerhoff et al., 2016)

3. Results

Aiming to improve the classical virotherapy, an epi-virotherapeutic approach combining oncolytic measles virus (MeV-GFP) and the HDACi resminostat on four aggressive pancreatic cancer cell lines was investigated in the following experiments.

At first, pancreatic cancer cell lines were evaluated for their sensitivity towards each agent in monotreatment. In these experiments the concentrations and MOIs were determined that were employed in combined epi-virotherapeutic experiments. Therefore, suitable dosages were defined leading to a remaining cell mass of 70-80% 96 hpi. After having found required concentrations, combination SRB cell viability assays were performed. The xCELLigence system was afterwards employed in order to confirm and further obtain more precise data regarding cooperative effects over the entire treatment period.

To further elucidate underlying synergistic mechanisms, it was examined whether virus growth kinetics could be altered by concomitant treatment with resminostat. Then, it was investigated whether resminostat´s pharmacodynamic function is potentially impaired in MeV-GFP-infected pancreatic cancer cells. Finally, resminostat-related modulation of MeV-GFP-induced activation of interferon(IFN)-signaling as a potential therapeutic target was analyzed.

3.1. Analysis of cytoreductive effects induced by oncolytic measles virus and resminostat on pancreatic cancer cells

3.1.1. Resminostat-induced cytotoxic effects

To get an overview of the time and dose-dependent effects of resminostat on pancreatic cancer cells, SRB cell viability assays were performed, examining cytoreductive effects of six ascending concentrations of resminostat (MOCK, 0.5, 1, 2.5, 5, 10 µM) at four

consecutive time points (24, 48, 72 and 96 hours post treatment (hpt)).

After having seeded cancer cells the day before, medium was removed and resminostat diluted within 500 µl medium (DMEM plus 10% FCS) was added. The remaining cell mass was quantified by SRB viability assays at 24, 48, 72 and 96 hpt.

Treatment with resminostat resulted in a dose- and time-dependent reduction of cell mass in all four tested pancreatic cancer cell lines. With the exception of MIA PaCa-2, all other cell lines did not exhibit a reduction in cell mass 24 hpt (Fig. 15). The other three cell lines featured a reduction in cell mass not until 48 hpt, indicating that resminostat-related cell death typically is induced between 24 and 48 hpt.

Whereas cell viability of BxPC-3 and MIA PaCa-2 cells (Fig. 15) did not further decrease between 72 and 96 hpt, a decrease in cell masses of AsPC-1 as well as PANC-1 was still observed. This implies that the period of cytoreductive effects of resminostat seems to vary between cell lines, irrespective of concentrations.

„

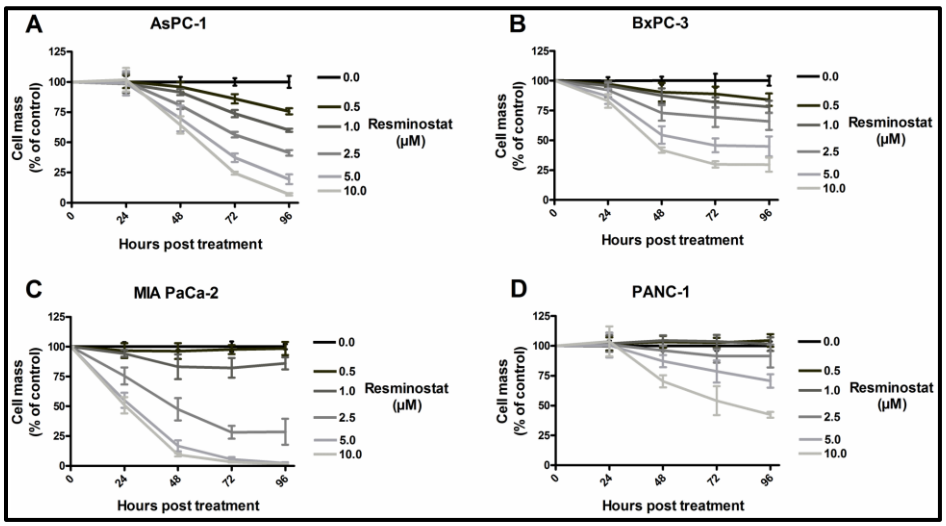

Figure 15: Evaluation of resminostat-induced pancreatic cancer cell mass reduction
Monotreatment with the epigenetic compound resminostat resulted in a dose- and time-dependent reduction of tumor cell masses in all tested pancreatic cancer cell lines (AsPC-1, BxPC-3, MIA PaCa-2 and PANC‑1). Six concentrations of resminostat (ranging from 0

to 10 µM) were administered and tumor cell viabilities were determined at four different time-points (24, 48, 72 and 96 h after treatment) utilizing a Sulforhodamine B (SRB) viability assay. Tumor cell masses are given in % of the mean of mock-treated tumor cells (resminostat concentration of 0 µM) for each time-point. Means and SDs of three independent experiments are shown." (Ellerhoff et al., 2016)

MIA PaCa-2 was the cell line that exhibited the earliest detectable reduction in cell mass and was also the most sensitive cell line. The conspicuous skip of cell mass between 1 µM and 2.5 µM resminostat is unique, as there is no similar feature in the results of other cell lines. In particular, resminostat concentrations of 0.5 and 1 µM led to a reduction in cell mass up to 10 %, whereas 2.5 µM of resminostat even elicited a reduction of about 70 %. Treatment with the next higher concentration of 5 µM almost killed all seeded cells at 96 hpt.

By contrast, PANC-1 cells were shown being most resistant towards resminostat. 70% of its cell mass remained at 96 hpt despite being exposed to the relatively high concentration of 5 µM of resminostat (Fig. 15).

Taking the two other cell lines into account, BxPC-3 cells were more resistant than AsPC-1 cells. Comparing cell viability at a concentration of 2.5 µM, remaining cell masses of 65% of BxPC-3 and 40% of AsPC-1 were obtained at 96 hpt.

3.1.2. MeV-induced cytotoxic effects

After having quantified the cytotoxic potency of resminostat, MeV-GFP was examined for its time- and dose-dependent cytoreductive effects on pancreatic cancer cells by applying a series of ascending MOIs.

Following the infection scheme described above, cell mass was determined at 72 and 96 hpi. In contrast to the SRB experiments with resminostat, both earlier time points 24 and 48 hpi were not examined this time. The rationale behind this procedure is based on the fact that previous experiments from our laboratory have already revealed that MeV-mediated oncolysis takes more time as

compared to classical cytotoxic drugs, since viruses have to initially occupy the synthetic machinery of host cells and cancer cells die only after several rounds of viral replication due to the induction of immunogenic cell death or self-induced apoptosis, respectively.

Cell lines were infected at different MOIs, depending on their susceptibility toward virus-mediated oncolysis. Consequently, MeV-GFP was characterized by a broader spectrum of efficiency than resminostat with respect to the distinct treated tumor type. After having infected cells at a MOI of 1.0, there were 50% of PANC-1 cells as compared to the MOCK-treated control, whereas there were 75% of BxPC-3 cells and more notable, cells from both other cell lines remained unaffected at 96 hpi (Fig. 16 B and D).

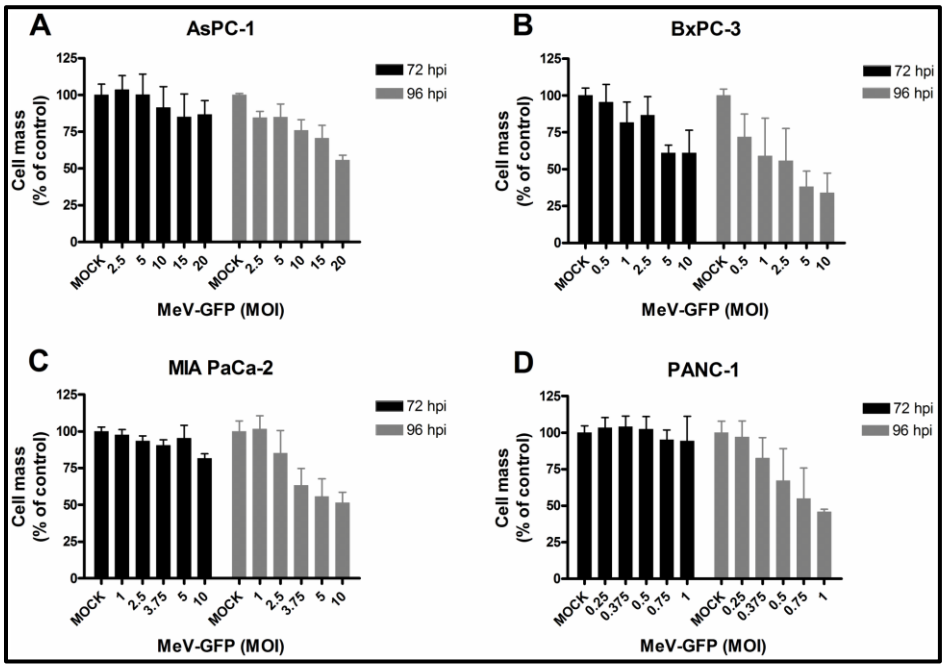

Figure 16: Evaluation of MeV-GFP-induced pancreatic cancer cell mass reduction
Mono-treatment with recombined measles virotherapeutics (MeV-GFP) resulted in a dose- and time-dependent reduction of tumor cell masses in all pancreatic cancer cell lines (AsPC-1, BxPC-3, MIA PaCa-2 and PANC-1). Virotherapeutic treatments were performed at indicated multiplicities of infection (50), being adjusted to the oncolytic susceptibility of the respective tumor cell line. Tumor cell viabilities were determined at 72 and 96 h post-infection (hpi) using SRB viability assays. Tumor cell masses are given in % of the mean of mock-treated tumor cells for each time-point. Means and SDs of three independent experiments are shown.

Nonetheless, as shown for resminostat treatment, the extent of MeV-GFP-mediated oncolysis was shown to be dose- and time-dependent.

“The tumor cell line being most sensitive to MeV‑GFP-mediated oncolysis was PANC‑1 (Fig. 16 D), whereas AsPC-1 tumor cells (Fig. 16 A) were found to be most resistant. Considering this, more than 50% of AsPC-1 cells survived virus infections at a MOI of as high as 20. In contrast, a tumor cell mass reduction of 50% was obtained by infecting PANC‑1 cells at a MOI of as low as 1.” (Ellerhoff et al., 2016)

As was already shown in several previous studies, MeV-GFP-induced oncolysis was initiated at later time points as compared to the cytoreductive effects of resminostat. In the case of PANC-1 cells, a measurable effect in comparison to the MOCK-treated control cells could not be detected until 96 hours. Cells of the other three cell lines exhibited a reduction in cell mass at 72 hpi which decreased further until 96 hpi. One explanation for the decrease in cell mass starting only at 96 hours after MeV-GFP infection may be deduced from the lowest MOIs, being applicated to PANC-1. Nonetheless, no decrease in cell viability could be detected 72 hpi after having been infected at a MOI of 1 whereas cell mass was remarkably reduced by over 50% during the following 24 hours.

“Addressing the question whether there is cross-resistance between resminostat and MeV‑GFP, a remarkable trend could be observed. Tumor cell lines, which had been identified to be more resistant toward resminostat exhibited a relatively strong sensitivity toward MeV‑GFP-mediated oncolysis and vice versa. The largest difference in tumor cell susceptibility was obtained in experiments with the PANC‑1 tumor cell line being most resistant against resminostat treatment, but most sensitive towards MeV‑GFP-mediated oncolysis (Figs. 2D and 3D).” (Ellerhoff et al., 2016)

3.1.3. Comparison between cytoreductive effects of MeV-GFP- or resminostat-monotreatment and epi-virotherapeutical treatment

"To further determine whether resminostat and oncolytic MeV operate beneficially when administered in combination, pancreatic cancer cells were initially infected with MeV‑GFP; then, resminostat was added following the regular change of infection culture medium at 3 hpi (Fig. 17). Tumor cell line adjusted MOIs of MeV‑GFP and concentrations of resminostat were used as determined prior in the monotherapy settings."(Ellerhoff et al., 2016)

"

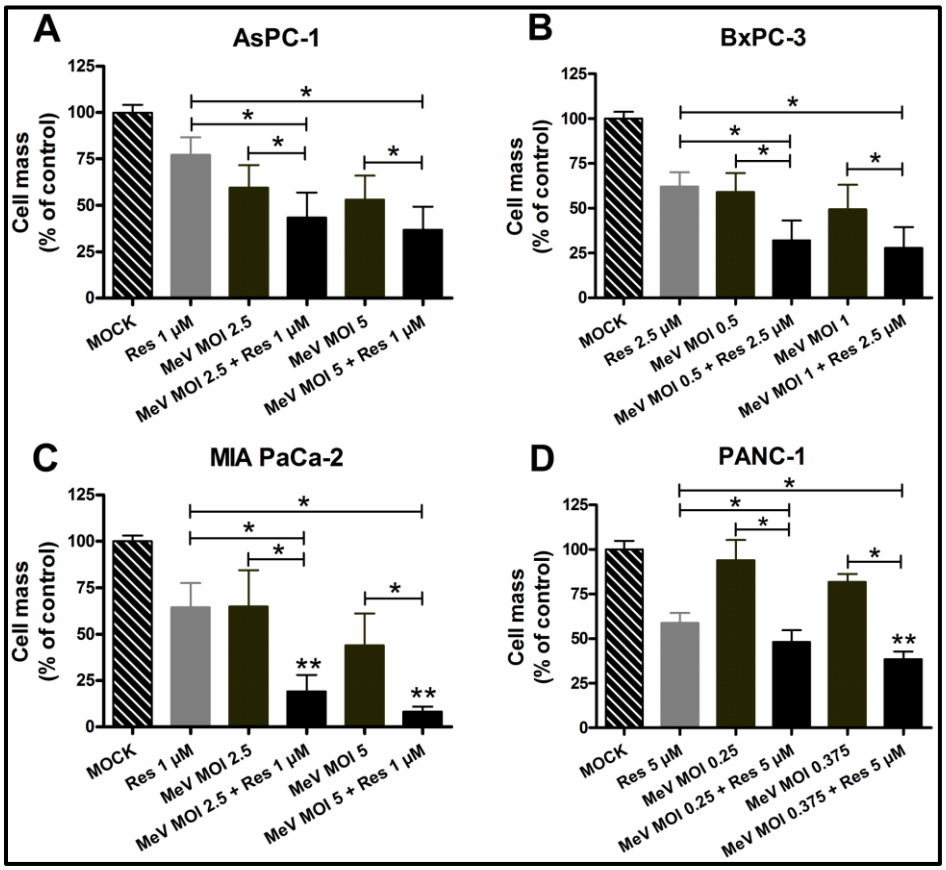

Figure 17: Epi-virotherapeutic treatment is superior to any corresponding monotherapy

Tumor cells were infected with MeV‑GFP (MeV) at indicated multiplicities of infection (50), being adjusted to the oncolytic susceptibility of the respective tumor cell lines. At 3 h post infection (hpi), resminostat was added at the indicated concentrations. Remaining tumor cell masses were determined at 96 hpi using SRB viability assays. Means and SDs of three different experiments are shown. *P-value <0.01 of ANOVA on logarithms of tumor cell mass in % of control, comparing epi-virotherapeutic treatment with monotreatment of

resminostat (Res) and MeV. **P-value <0.01 of interaction term in ANOVA verifying a more than additive (synergistic) effect." (Ellerhoff et al., 2016)

"As a result, supplementation of oncolytic MeV-GFP by resminostat resulted in beneficial effects on rates of tumor cell mass reduction in all tested pancreatic cancer cell lines. With regard to MOIs of MeV-GFP and concentrations of resminostat employed in later experiments, the reduction in tumor cell mass could be amplified from 53 to 37% for AsPC-1 (MOI 5), from 60 to 32% for BxPC-3 (MOI 0.5), from 65 to 19% for MIA PaCa-2 (MOI 2.5), and from 93 to 48% for PANC-1 (MOI 0.25) (Fig. 17). Considering that HDACi *per se* induce a reduction in pancreatic cancer cell masses, the most striking benefit could be obtained in the treatment of MIA PaCa-2 cells, achieving a further 45% reduction in tumor cell mass (Fig. 17 C, comparison of bars 2 and 6). Whereas both agents in monotherapy reduced tumor cell viability each by 35% in comparison to the mock control, the combination led to a tumor cell mass reduction of >80% in comparison to the mock control (Fig. 17 C, comparison of bars 1 and 6). A statistical analysis was carried out to investigate whether an interaction between MeV-GFP and resminostat is verifiable that caused a more pronounced effect on tumor cell mass reduction than expected from a simple additive effect. The interaction term in the ANOVA on the logarithms of tumor cell mass in % of control confirmed a clear significant synergistic antitumor effect for the treatment of MIA PaCa-2 cells (Fig. 17 C) as compared to the cytotoxic effect that would be expected from an additive effect. With regard to the other pancreatic cancer cell lines, synergistic tumor cell killing could be significantly revealed in PANC-1 cells for only one of the two combinations (MeV MOI 0.375 and 5 µM resminostat; Fig. 17 D); in contrast, no synergistic effects were found for AsPC-1 and BxPC-3 tumor cells (Fig. 17 A and B), suggesting that the epi-virotherapeutic approach

does not elicit synergistic effects in all pancreatic cancer cell entities, presumably as a result of tumor cell specific features." (Ellerhoff et al., 2016)

„

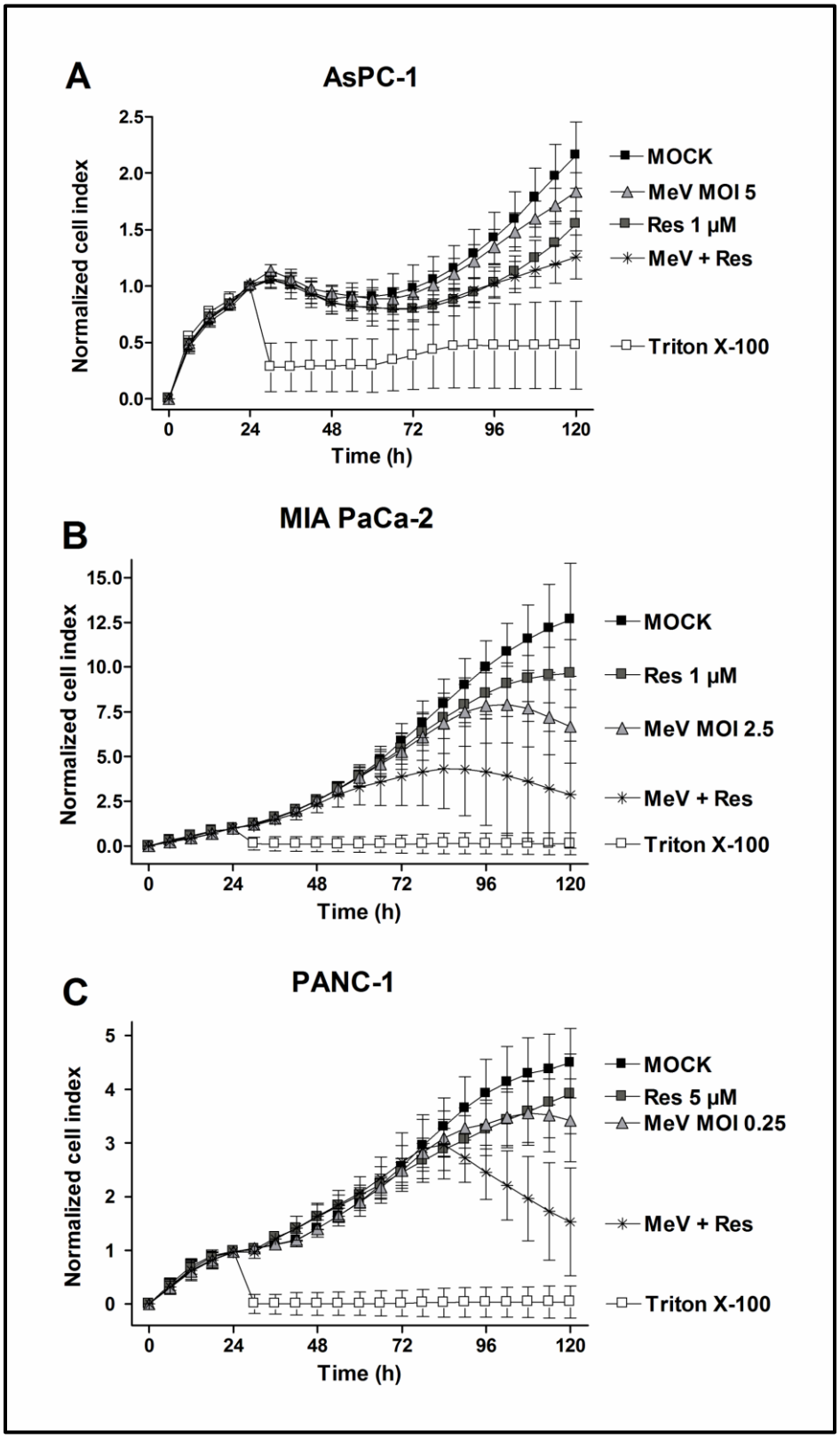

Figure 18: Detailed analysis of pancreatic cancer cell viability over 120 h of epi-virotherapeutic treatment.

Beneficial effects of epi-virotherapeutic co-treatment were confirmed and specified by real-time proliferation monitoring providing tumor cell viability data over the entire treatment period of 120 h. Following the initial tumor cell seeding (at hour 0), three of the four pancreatic cancer cells (AsPC-1, MIA PaCa-2 and PANC-1) were infected 21 h later with recombined measles virotherapeutics (MeV-GFP) at MOIs used in SRB combination-experiments or not treated (mock); then, at three hours post-infection, tumor cells were treated with the epitherapeutic compound resminostat (Res) at indicated concentrations. Treatment with Triton X-100 1%, inducing maximum tumor cell lysis, was used as a negative control. Cellular impedance was measured continuously using the xCELLigence SP system. Depicted are the data obtained in 6-h intervals. Cell index was normalized after 24 h when treatment had been accomplished (additional administration of resminostat or Triton X-100). Means and SDs of three different independent experiments are shown." (Ellerhoff et al., 2016)

"To confirm our results from the SRB viability assays and to gain more precise information on the entire treatment time course, real-time pancreatic cancer cell proliferation was determined using the xCELLigence system (Fig. 18). The acquired data revealed that our epi-virotherapeutic treatment elicited beneficial effects on tumor cell viabilities in three out of the four tested pancreatic cancer cell lines (Fig. 18). Taken together, these findings underline that: i) our specific epi-virotherapeutic treatment is much more valuable for MIA PaCa-2 and PANC-1 tumor cells than for AsPC-1 cells (BxPC-3 tumor cells were not included in this specific testing) and ii) the mode of synergistic tumor cell killing is first observed at 72 hpi in all tested pancreatic cancer cell lines (going along with MeV-mediated oncolysis phenomena taking place at this time-point)." (Ellerhoff et al., 2016)

In conclusion, epi-virotherapeutical treatment could elicit boosted anti-tumor effects in all pancreatic cancer cell lines. However, the extent differed from cell line to cell line, confirming solely a statistically significant synergistic interaction at both examined time points for MIA PaCa-2 cells. The presented results raise the questions whether there might be underlying molecular mechanisms explaining the synergistic mode of action or whether both agents work independently from each other. For this reason, virus growth kinetics were investigated in a further step with the aim

of assessing whether MeV-GFP replication and spread is possibly amplified by co-treatment with resminostat.

3.2. Impact of epi-virotherapeutical treatment on measles growth kinetics in pancreatic cancer cells

"To further determine whether resminostat and oncolytic MeV operate beneficially when administered in combination, pancreatic cancer cells were initially infected with MeV-GFP; then, resminostat was added following the regular change of infection culture medium at 3 hpi. Tumor cell line adjusted MOIs of MeV-GFP and concentrations of resminostat were used as determined prior in the monotherapy settings." (Ellerhoff et al., 2016)

3.2.1. Analysis of MeV-GFP growth kinetics in pancreatic cancer cells

At first, virus growth characteristics were investigated in the four pancreatic cancer cell lines without co-treatment with resminostat (Fig. 19).

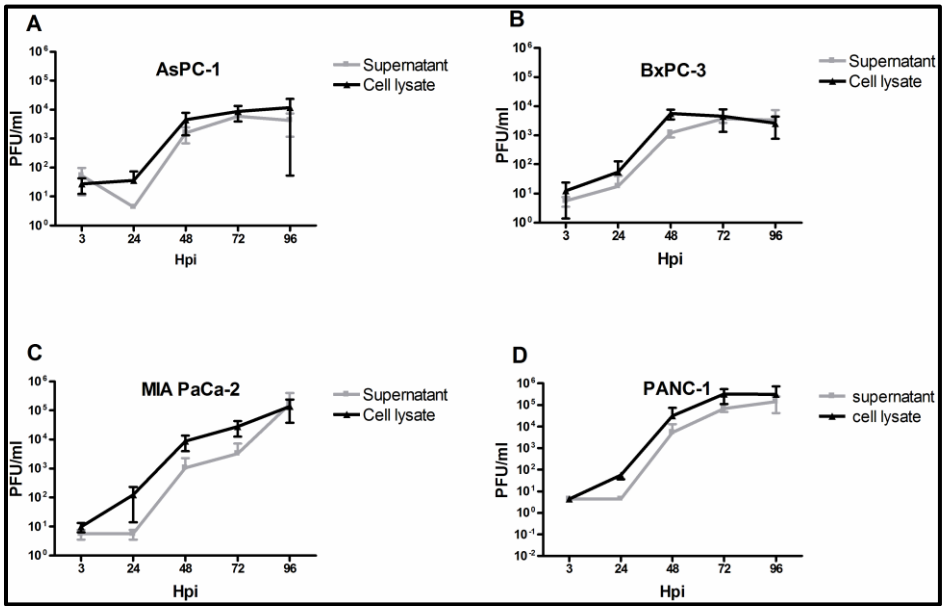

Figure 19: Virus growth curves of pancreatic cancer cells infected with MeV-GFP
Tumor cells were infected at different MOIs. AsPC-1 at 5, BxPC-3 at 0.5, MIA PaCa-2 at 2.5 and PANC-1 at 0.25. Samples were taken at 3, 24, 48, 72 and 96 h post-infection (hpi). Tumor cell lysates (curves to the left, solid lines) provide information on viral particles being

found in intact tumor cells, whereas supernatant samples (curves to the right, dotted lines) reflect the release of newly generated infectious MeV-GFP particles from tumor cells. Results were obtained by virus titration on Vero cells. Displayed are means and SDs of three independent experiments. pfu, plaque forming unit; hpi, hours post-infection."

Similar features could be identified in all tested pancreatic cancer cell lines. The amount of virus both released and cell-associated did not start increasing until 24 hpi and reached a plateau at around 72 hpi or even started decreasing three days post infection in case of BxPC-3 cells. The highest virus titers were reached in PANC-1 and MIA PaCa-2 cells (Fig. 20 C and D), amounting 10^5 PFU/ml whereas in AsPC-1 and BxPC-3 only 10^4 PFU/ml were detected (Fig. 19 A and B).

Comparing the viral titers in supernatants and in cell lysates, viral concentrations in cells were almost equal to those in medium. This was found in all four pancreatic cancer cell lines.

With regard to the quantity of virus titers, it might be expected that cell lines infected at higher MOIs should produce higher titers in comparison to cell lines infected at lower MOIs. AsPC-1 cells that were infected at the highest MOI (5), did not yield the highest viral titer (Fig. 19 A). Nonetheless, primary viral titers (3 hpi both in cell lysates and supernatants) were the highest among all four pancreatic cancer cells as might be deduced from the highest MOI. AsPC-1 and BxPC-3 cells were seeded at higher densities compared to the other two cell lines but did not reach the highest virus titers (Fig. 19 A and B). Likewise, no clear correlation between the sensitivity towards MeV-GFP-mediated oncolysis and the amount of detected viruses could be observed. As a proof, BxPC-3 cells were shown to be more sensitive than MIA PaCa-2 cells but yielded lower MeV-GFP virus titers (Fig. 19 B and C).

SRB assays had revealed that MeV-mediated oncolysis did not occur until 72 hpi, suggesting that virus release should emerge around this time point. In contrast to this consideration, great amounts of MeV-GFP were already released 48 hpi, indicating that

MeV first occupies the synthetic machinery and subsequently forces host cells to produce viral progenies. Finally, after having created a great amount of progenies, the synthetic machinery of host cancer cells collapses and consequently cells are compelled to initiate apoptosis.

3.2.2. Comparison of MeV-GFP growth kinetics in presence and absence of resminostat in pancreatic cancer cells

„

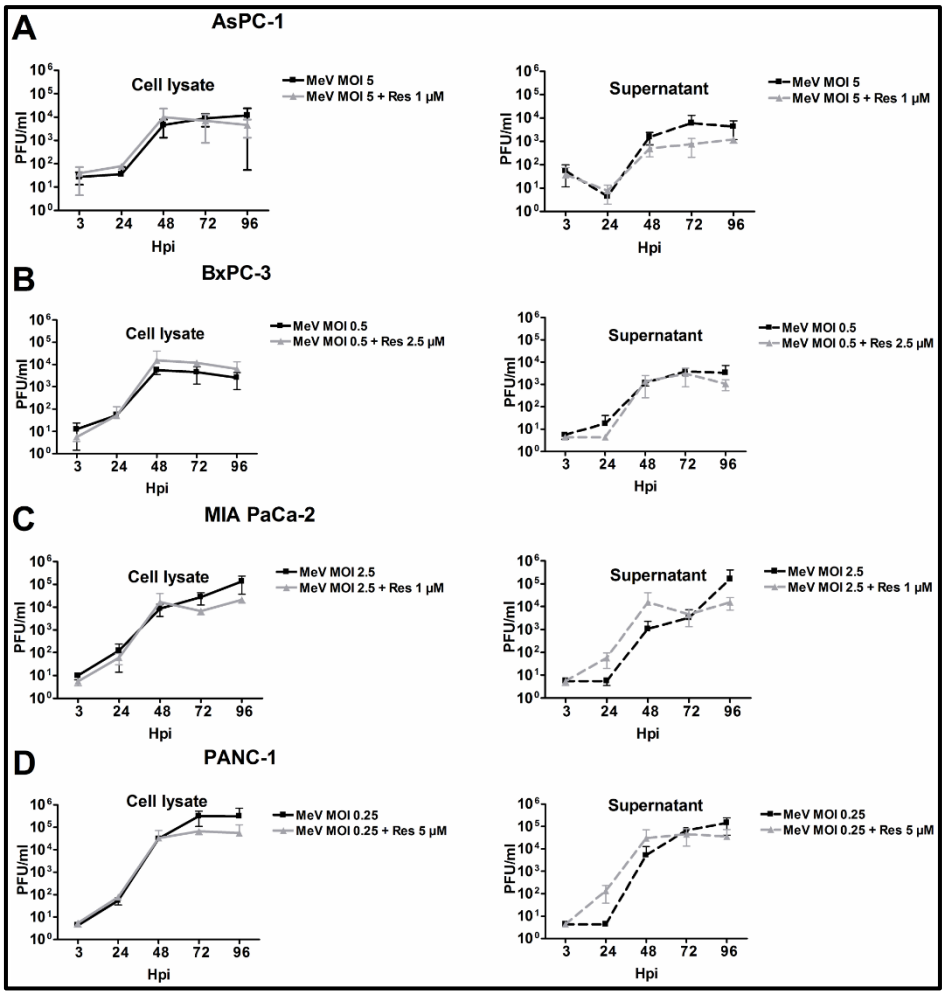

Figure 20: Resminostat co-treatment did not alter MeV-GFP growth kinetics

Virus growth curves of well characterized pancreatic cancer cell lines did not exhibit significant differences of measles virotherapeutic replication when being determined in absence or in presence of the epigenetic compound resminostat. Tumor cells were co-treated with MeV-GFP (MeV) and resminostat (Res) at stated multiplicities of infection (MOIs) and concentrations of the epigenetic compound (µM). Samples were taken at 3, 24, 48, 72 and 96 h post-infection (hpi). Tumor cell lysates (curves to the left, solid lines) provide information on viral particles being found in intact tumor cells, whereas

supernatant samples (curves to the right, dotted lines) reflect the release of newly generated infectious MeV‑GFP particles from tumor cells. Results were obtained by virus titration on Vero cells. Displayed are means and SDs of three independent experiments. pfu, plaque forming unit; hpi, hours post-infection." (Ellerhoff et al., 2016)

Next, MeV-GFP growth kinetics were determined in presence of resminostat and compared to those obtained by monotreatment with MeV-GFP. In respect of the curve shapes of epi-viro-therapeutical treatment, no significant differences were obtained when compared to those growth curves obtained by MeV-GFP-infected pancreatic cancer cells (Fig. 20).

"At later time-points (at 72 and 96 hpi) viral titers were slightly lower in supernatants as well as in tumor cell lysates in the presence of resminostat. This may be due to a greater tumor cell mass reduction induced by the combination treatment at later time-points, so that fewer tumor cells were present in the cultures at these later time-points resulting in a significantly lower cellular capacity for production of viral progeny particles. In conclusion, enhanced oncolytic effects by the combined treatment of MeV‑GFP and resminostat were not found to be caused by an enhancement of viral replication by the HDACi." (Ellerhoff et al., 2016)

3.3. Analysis of pharmacodynamic function of resminostat in MeV infected pancreatic cancer cells

"Decrease in the expression of zinc finger protein 64 (zfp64) has been revealed to be a good surrogate parameter for the pharmacological activity of resminostat. Therefore, we examined mRNA expression of zfp64 after monotreatment with either resminostat or MeV‑GFP and after combination treatment (resminostat plus MeV‑GFP) using the same resminostat concentrations and MOIs as in all prior experiments (Fig. 21). In the presence of resminostat, zfp64 expression was found to be

downregulated in each tumor cell line as early as after five hours of treatment initiation. Under epi-virotherapeutic co-treatment with resminostat and MeV-GFP, we still observed a lower expression of zfp64 as compared to the mock-treated control (with AsPC-1 tumor cells showing an even lower expression under co-treatment as compared to resminostat treatment alone; Fig. 21 A).

„

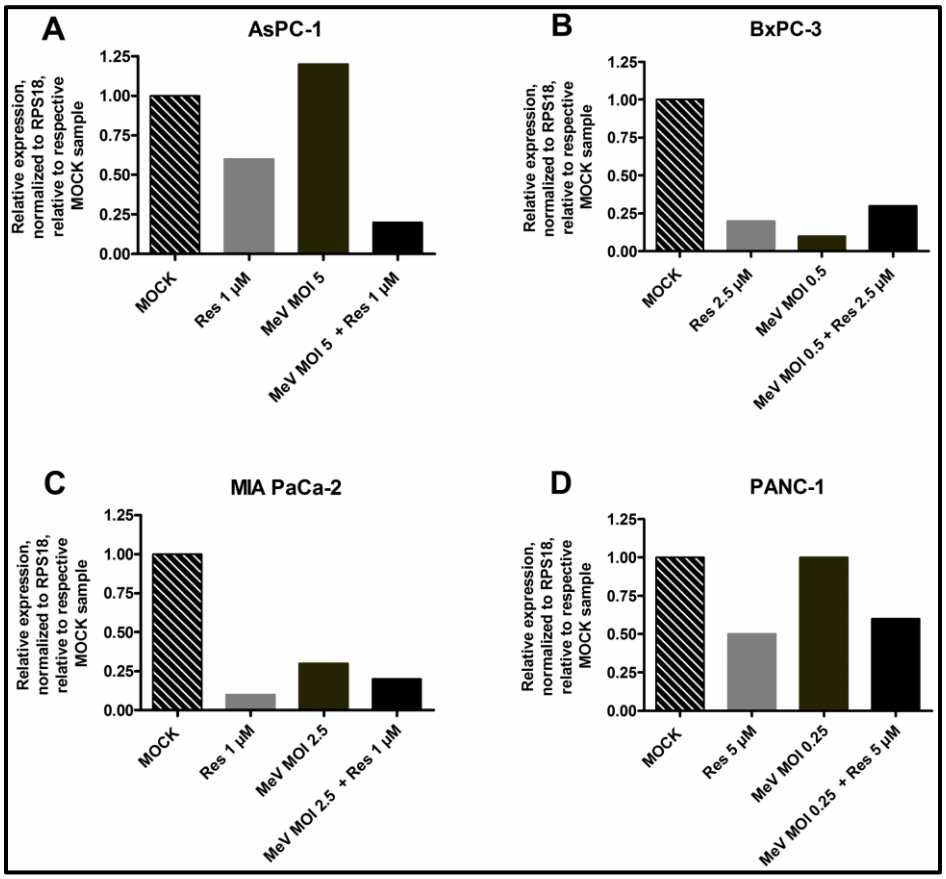

Figure 21: Analysis of the resminostat pharmacodynamic function in MeV-GFP-infected pancreatic cancer cells
Unimpairment of the resminostat (Res) pharmacodynamic function in pancreatic cancer cells being infected with recombined measles virotherapeutics (MeV-GFP) was deduced from the decrease in expression of zinc-finger protein 64 (zfp64) after 5 h of epigenetic treatment. Tumor cells were infected with MeV-GFP at stated MOIs and co-treated with indicated concentrations of resminostat starting at 3 h post-infection. RNA samples were obtained after 5 h of treatment. Expression levels of zfp64, representing a well-defined surrogate parameter for the epigenetic impact of resminostat, were determined using RT-qPCR. Values were normalized to the housekeeping gene RPS 18 (ribosomal protein S18), and relative expression is displayed compared to corresponding control samples (mock; no infection with MeV-GFP and no treatment with resminostat). Data of a representative experiment are shown. MeV + Res, co treatment with measles virus MeV-GFP and resminostat with concentrations and MOIs as used in the respective mono-treatment experiments." (Ellerhoff et al., 2016)

In contrast, different expression patterns of zfp64 were found when tumor cells had only been infected with MeV-GFP; in these cases, zfp64 was only downregulated in BxPC-3 and MIA PaCa-2 tumor cells (Fig. 21 B and C), but there was no detectable regulation in AsPC-1 and PANC-1 tumor cells (Fig. 21 A and D). In conclusion, our experiments provide evidence that the pharmacodynamic function of resminostat did not seem to be impaired in MeV-GFP-infected pancreatic cancer cell lines." (Ellerhoff et al., 2016)

3.4. Impact of resminostat on MeV-GFP-activated JAK/STAT signaling in pancreatic cancer cells

"In most studies investigating epi-virotherapeutic approaches so far, damping of the anti-viral response by HDACi was highlighted as a potential explanation for underlying synergistic antitumoral effects of this combined treatment approach. Accordingly, we were interested in the functionality of IFN-signaling of pancreatic cancer cells in the presence and absence of resminostat during infections with MeV-GFP." (Ellerhoff et al., 2016)

For this reason, phosphorylation of STAT1 and expression of the IFN-stimulated-gene (ISG) IFIT1 were investigated by immuno-blotting. STAT1 gets phosphorylated after binding of IFN to its receptor causing hetero- and homodimerisation, thereby forming a complex with STAT2 and IRF9 which subsequently enters the nucleus with the objective of initiating transcription of ISGs (Schneider et al., 2014). One of the emerging ISGs is IFIT1, being assigned for detection of viral RNA as well as binding and inactivating of viral pathogenic proteins (Diamond and Farzan, 2013). To ensure that proteins were loaded in equal amounts, membranes were additionally incubated with antibodies against STAT and β-actin.

3.4.1. Analysis of JAK/STAT-signaling after MeV-GFP infection

Since approximately 80% of cancer cells have lost their ability of producing a proper IFN-mediated antiviral response (Stojdl et al., 2003), it was first investigated whether pancreatic cancer cells have the ability of activating IFN signaling due to MeV-GFP infection.

As a phosphorylation of STAT1 and an expression of IFIT1 were observed in AsPC-1, BxPC-3 and PANC-1 cells at 72 hpi it is in all probability suggested that activation of IFN signaling functioned appropriately in these cell lines. In contrast, neither phosphorylation of STAT1 nor expression of IFIT1 were detectable in MIA PaCa-2 cells (Fig. 22), being indicative of defects in the IFN-signaling pathway of those cells.

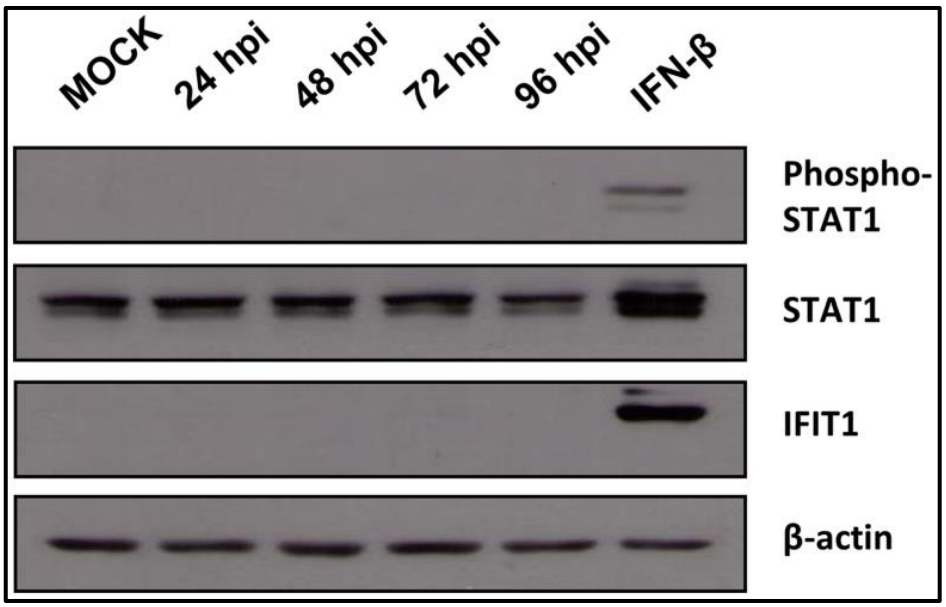

Figure 22: MeV-GFP did not induce IFN signaling in MIA PaCa-2 cells
Tumor cells were either infected with MeV-GFP (MOI 2.5) or treated without infection (mock); then, samples were taken at 24, 48, 72 and 96 hours post-infection (hpi) and analyzed by immunoblotting; tumor cells stimulated with interferon-β (IFN-β) were used as positive controls. Potential activation of IFN signaling by MeV-GFP was deduced from phosphorylation of STAT1 (phospho-STAT1) and expression of interferon-induced protein with tetratricopeptide repeats 1 (IFIT1). β-actin was used as a loading control." (Ellerhoff et al., 2016)

3.4.2. Analysis of JAK/STAT-signaling after co-treatment with MeV-GFP and resminostat

"We then investigated the impact of resminostat on MeV-GFP-induced activation of IFN signaling in AsPC-1, BxPC-3, and PANC-1 cells. As a result, resminostat monotreatment did neither result in phosphorylation of STAT1 nor in expression of IFIT1.

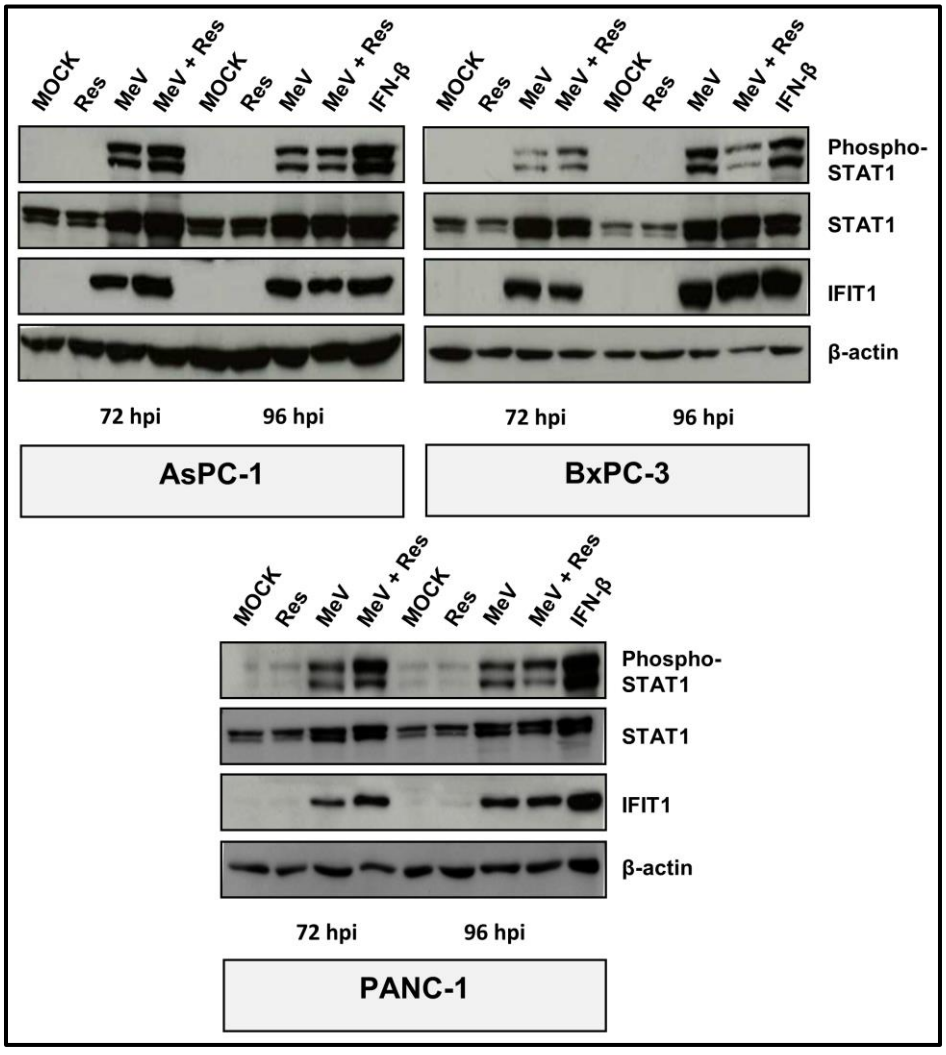

Figure 23: Resminostat does not impair MeV-induced activation of IFN signaling
AsPC-1, BxPC-3 and PANC-1 cells were mock-treated (mock), treated with resminostat (Res) or/and MeV-GFP (MeV) or not treated at all (mock). Stimulation with IFN-β for 24 h (IFN-β) served as a positive control. MeV-induced activation of IFN-signaling was revealed by phosphorylation of STAT1 (phospho-STAT1) and expression of IFIT1, being detected by immunoblotting. β-actin was used as a loading control.

However, both MeV-GFP infection alone as well as the epi-viro-therapeutic combination resminostat plus MeV-GFP were found to activate IFN signaling at both 72 and 96 hpi, indicated by phosphorylation of STAT1 and expression of IFIT1 (Fig. 23). As MIA PaCa-2 cells did not initiate IFN signaling after MeV-GFP infection, we stimulated these tumor cells with IFN-β (please note: BxPC-3 cells were used as a control in this experiment). Some of these were additionally treated with resminostat. As a result, IFN-β treatment was found to induce IFN signaling; but similar to all prior results, resminostat was unable to inhibit phosphorylation of STAT1 and expression of IFIT1 (Fig. 24). These results clearly imply that resminostat does not impair the IFN response of pancreatic cancer cells that had been initiated by infection with MeV-GFP. Consequently, resminostat does not elicit synergistic effects due to an impairment of the anti-viral response.

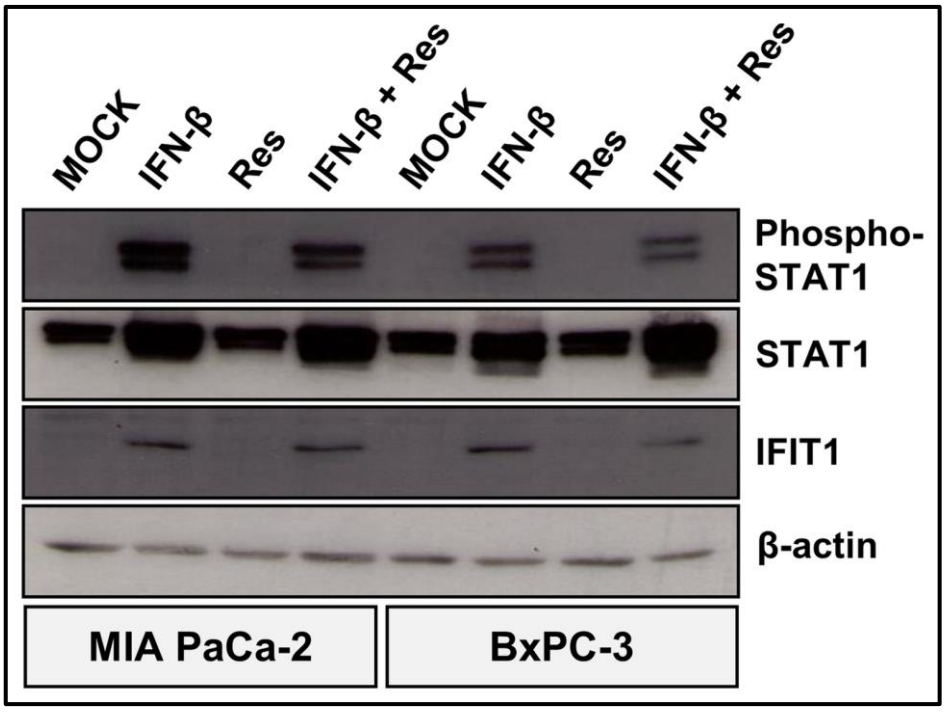

Figure 24: Resminostat does not impair IFN signaling in MIA PaCa-2 cells being exogenously stimulated by IFN

MIA PaCa-2 and BxPC-3 cells were treated with IFN‑β and/or resminostat (Res) for 24 h or not treated at all (mock). Potential impairment of IFN signaling by resminostat was deduced from phosphorylation of STAT1 (phospho-STAT1) and expression of interferon-induced protein with tetratricopeptide repeats 1 (IFIT1). β-actin was used as a loading control." (Ellerhoff et al., 2016)

4. Discussion

"Oncolytic viruses have recently made a major move toward their full establishment in clinical practice by approval of Imlygic® both by the American Food and Drug Administration (FDA) and by the European Medicines Agency (EMA) (Ledford, 2015). In our study, an epi-virotherapeutic approach was pursued, augmenting oncolytic MeV with the oral HDACi resminostat.

Both agents already have been evaluated independently as well as recently in combination for the treatment of different solid tumors with encouraging results (Russell et al., 2012, Nguyen et al., 2010, Ruf et al., 2015, Brunetto et al., 2013, Abend and Kehat, 2015, Mottamal et al., 2015, Feng et al., 2014, Xu et al., 2013). Here, we tested a series of four human pancreatic cancer cell lines: i) for their sensitivity to both agents in monotreatment and subsequently ii) toward the effect of epi-virotherapeutic co-treatment.

At the outset, monotreatment experiments revealed that both agents, oncolytic MeV-GFP as well as resminostat, caused dose- and time-dependent tumor cell killing in all tested human pancreatic cancer cell lines. Strikingly, the cytotoxic effect of resminostat on a specific cancer cell line could not be predicted from the results obtained in OV cytotoxicity assays and vice versa. This is most clearly visible when comparing the virotherapeutic with the epigenetic results obtained with PANC-1 cells emphasizing that there is no cross-resistance between OV and other cytotoxic drugs such as HDACi.

Subsequently, cooperative effects were evaluated by performing SRB cell viability assays and afterwards confirmed utilizing the xCELLigence system. The results showed that the epi-virotherapeutic approach elicited beneficial cytotoxic effects in all four pancreatic cancer cell lines. Regarding MIA PaCa-2 tumor cells, considerable synergistic results were observed: virus-mediated reduction in the tumor cell masses was found to be

improved in the presence of resminostat from 35 to 81% (at MOI 2.5) as well as from 55 to 92% (at MOI 5) (Fig. 17). Similarly, epi-virotherapeutic treatment of the other three cancer cell lines exhibited stronger effects than obtained in monotreatment. In further experiments we found that virus growth curves revealed no significant differences in the presence or absence of resminostat, suggesting that resminostat neither facilitated virus entry nor enhanced virus replication.

With regard to studies that have already investigated the therapeutic potential of epi-virotherapeutic treatment of different tumor entities, the most frequently examined and highlighted molecular mechanism of synergism is the ability of HDACi to impair the anti-viral immune response of host tumor cells, thereby facilitating virus replication and spread. Many underlying mechanisms have been revealed, describing involvement of HDAC activity in almost each step of IFN signaling. Virus infection leads to phosphorylation of IFN-regulatory factors (IRFs), homo- or heterodimerization and translocation into the nucleus where IFN-β expression is induced (Honda et al., 2006). Trichostatin A (TSA) was shown to prevent proper IRF-3 function, thereby hindering cells to produce IFN-β (Nusinzon and Horvath, 2006). Downstream signaling of the IFN-β receptor likewise requires HDAC activity, enabling proper receptor activation, STAT dimerization, and IRF-9 function as well as the formation of the IFN-stimulated gene factor-3 (ISGF3) (Genin et al., 2003, Tang et al., 2007, Yuan et al., 2005). Also, HDAC are involved in the expression of IFN-stimulated-genes (ISGs) (Chang et al., 2004). Accordingly, HDAC inhibitors were proven to impair the expression of ISGs when tumor cells were coincidently infected with oncolytic viruses (Otsuki et al., 2008, Shulak et al., 2014, Nguyen et al., 2008). Due to these findings, the enhanced oncolytic effect was retrospectively assigned to the interference with IFN signaling.

In contrast to these observations, the present epivirotherapeutic approach did not modulate IFN signaling as indicated by an unaltered phosphorylation of STAT1 and expression of the ISG IFIT1 in any of the tested pancreatic cancer cell lines. Moreover, no obvious alteration in virus growth kinetics could be observed. For these reasons, our experiments do not support the prevailing opinion of HDACi damping the IFN-response thus enhancing OV-mediated oncolysis. In respect of implementing our epi-virotherapeutic approach into clinical practice, it is potentially even not preferable that type I IFN production is impaired. Since especially IFN-α and IFN-β are essential cytokines that attract and prime cytotoxic and T helper cells by causing expression of important receptors on cancer cells (such as MHC I), type I IFN secretion from tumor sites might amplify an antitumor immune response (Fuertes et al., 2011, Prestwich et al., 2009).

Other studies having examined the potential of HDACi to enhance different virotherapeutics obtained similar findings. After having infected different infection-resistant cancer cells with vaccinia virus (VV) that had retained their B18R gene, functioning as an IFN antagonist, the HDACi TSA was still capable of amplifying OV-mediated oncolysis, suggesting that its antitumor effect was not based on an immunosuppressive function (MacTavish et al., 2010). In our study, MIA PaCa-2 was the only pancreatic cancer cell line which did not exhibit an activation of the IFN signaling pathway after MeV infection. Despite this lack of establishing a proper anti-viral state, it was not the most susceptible cell line to MeV-mediated oncolysis and more noteworthy, epi-virotherapeutic treatment showed the most pronounced effect in this cell line, stressing that HDACi seem to enhance virus-mediated oncolysis by eliciting other effects than damping the IFN response. This raises the question which additional mechanisms could explain the enhancement of virus-mediated cell death by epi-virotherapeutic co-treatment.

Explanations, amongst others, were provided by Liu *et al (Liu et al., 2008)*. Using an epi-virotherapeutic approach consisting of oncolytic herpes-simplex-virus (HSV) and TSA in a panel of tumor and normal quiescent cells, they obtained beneficial cytoreductive effects compared to monotreatment. These effects could be attributed neither to the dosing schedule nor to enhanced infectivity or virus replication. The authors rather ascribed the results to a decrease in expression of cyclin D1, mediating cell cycle arrest, and VEGF, reinforcing the hypothesis of vascular shutdown induced by OV (Breitbach et al., 2011).

Beyond the above, further replication-independent mechanisms have been illustrated, highlighting the impact of HDACi on cell signaling. Thus, HDACi cause hyperacetylation of NF-κB, thereby increasing its nuclear retention and DNA binding capacity. Due to its promotion of HSV gene expression, this HDACi-mediated effect elicited synergistic tumor killing in oral squamous cell carcinoma (SCC) cells (Katsura et al., 2009). Furthermore, combined treatment was shown to increase the expression of p21 which mediates cell cycle arrest, consequently slowing down tumor progression and resulting in the induction of tumor cell apoptosis.

Recently, Shulak *et al* found a mechanism explaining NF-κB activity accompanied by an enhanced OV-mediated oncolysis. They pointed out that hyperacetylation and nuclear retention of NF-κB induced the expression of several autophagy-related genes. They argued that the induction of autophagy led to an impairment of IFN signaling but also to vesicular stomatitis virus (VSV)-mediated apoptosis in prostate cancer cells (Shulak et al., 2014). Autophagy is a process that is *per se* frequently enhanced in tumor cells since it serves as a stress response to oxidative stress, lack of nutrients, and hypoxia as it is commonly present in the microenvironment of solid tumors (Murrow and Debnath, 2013). Interestingly, pancreatic cancer cells even require this catabolic process in order to prevent

accumulation of ROS, thereby contributing to tumor growth as well as establishing the basis for drug resistance (Yang et al., 2011, White and DiPaola, 2009)(64,65). Despite these pro-survival aspects, some viruses are notably capable of exploiting the autophagic machinery for the purpose of efficient replication (Dreux and Chisari, 2010). Attenuated MeV derived from the *Edmonston* strain actually induce and require autophagy for efficient replication (Richetta et al., 2013). Since hydroxamic acid based HDACi equally increase autophagic activity (Gammoh et al., 2012), it is tempting to speculate that the effect elicited by resminostat in combination with oncolytic MeV is caused by an enhanced self-digestion and subsequently enhanced tumor cell death.

Physiologically, cell signaling often requires protein modifications such as phosphorylation or acetylation but beyond targeting cell proteins, even pathogenic proteins can serve as substrates for those modifications, resulting either in enhanced or impaired activity. In this context, it was revealed that a portion of the NS-1 protein, representing the major pathogenic and most important protein for replication of the rat parvovirus H-1PV, gets acetylated during virus infection (Hristov et al., 2010). Noteworthy, treatment with VPA caused hyperacetylation of NS-1 resulting in an accumulation of ROS and an enhanced transcriptional activity. Ultimately, DNA damage in cancer cells was observed consequently inducing apoptosis. Those findings were confirmed later *in vivo*, resulting in complete disappearance of implanted tumors in mice that had undergone co-treatment with H-1PV and VPA (Li et al., 2013). Likewise, HDACi-related hyperacetylation of microtubules accelerated nuclear translocation of oncolytic HSV-genomes, thereby enhancing the antitumor effect in glioma stem-like cells (Nakashima et al., 2015a).

In conclusion, our results provide evidence that the epivirotherapeutic combination of oncolytic MeV and the HDACi resminostat

constitutes a beneficial option in the treatment of advanced pancreatic ductal adenocarcinoma. We revealed an augmentation of MeV-mediated oncolysis by resminostat. Treatment of MIA PaCa-2 cells resulted even in a synergistic enhancement of the tumor-killing potential when compared to the monotherapies. Molecular mechanisms underlying the synergistic effects and the potential of our epi-virotherapeutic approach *in vivo* have to be elucidated in animal models in the future.” (Ellerhoff et al., 2016)

5. Summary

Since the beginning of the 19th century researchers have tried to cure cancer patients with the aid of virus infection. Due to the present developments of genetic modifications with the possibility of generating a specific tumor tropism and the clinical establishment of the first oncolytic virus, the field of virotherapy is of great interest. To overcome existing limitations of virotherapeutics and to further enhance the antitumor efficiency of oncolytic viruses, the present study was conducted to examine the therapeutical potential of an epi-virotherapeutic approach combining oncolytic measles virus with the oral Histone-Deacetylase-Inhibitor resminostat on a panel of human pancreatic cancer cell lines.

After having determined the antitumor potential of each agent in monotreatment, SRB cell viability assays revealed that epi-vio-therapeutic treatment elicited much stronger cytotoxic effects than single-agent treatment on the four human pancreatic cancer cell lines. Those were partly stronger than those that would be statistically expected from an additive effect.

These results were subsequently confirmed and specified by performing real-time tumor cell proliferation assays (xCELLigence). Preparation and analysis of virus growth curves showed that virus replication and spread exhibited similar growth kinetics regardless of whether resminostat had been additionally applied or not.

Furthermore, analysis of the surrogate parameter zfp64 confirmed that resminostat is not impaired in its pharmacodynamic function in human pancreatic cancer cells that had been infected with measles virus.

The most highlighted molecular synergistic working point is the ability of HDACi to impair the antiviral immune response of cancer cells leading to enhanced virus replication and consequently to enhanced virus-mediated oncolysis. In contrast, our immunoblot analysis of the resminostat-based modulation of virus-induced IFN-

signaling activation, represented by phosphorylation of STAT1 and the expression of IFIT1, revealed no difference whether human pancreatic cancer cells had been treated additionally with resminostat or not.

In conclusion, our data show that epi-virotherapeutical treatment of human pancreatic cancer cells is beneficial when compared to either of the mono-agent treatments. Furthermore, it is suggested that oncolytic measles and resminostat seem to act independently. Future studies should investigate the anti-tumoral potential of the epi-virotherapeutic approach in vivo which should also serve to find underlying molecular mechanisms of synergy.

6. Zusammenfassung

Bereits zu Beginn des 19. Jahrhunderts versuchten Wissenschaftler Tumorpatienten mithilfe von Virusinfektionen zu heilen. Im Zuge der Möglichkeit, Viren genetisch zu modifizieren, einen definierten Tumortropismus zu erzeugen und der aktuell erfolgreichen Anwendung an Patienten mit malignem Melanom erlangte das Forschungsfeld der Virotherapie in den letzten Jahren großes Interesse.

Die vorliegende Studie wurde durchgeführt, um bestehende Limitationen der Virotherapie zu adressieren und weiterhin die antitumorale Effizienz onkolytischer Viren zu verbessern. Der dabei gewählte Ansatz bestand aus einer Kombination von onkolytischen Masern-Impfviren und dem oral applizierbaren Histon-Deacetylase-Inhibitor (HDACi) Resminostat, welcher auf seinen anti-tumoralen Effekt an vier verschiedenen humanen Pankreaskarzinomzelllinien untersucht wurde.

Nachdem zunächst das zytoreduktive Potential jedes einzelnen Kombinationspartners untersucht worden war, zeigten die SRB Zellviabilitäts-Assays, dass der epi-virotherapeutische Ansatz in allen vier humanen Pankreaskarzinomzelllinien dem jeweiligen Monotherapie-Ansatz überlegen war. Die anti-tumoralen Effekte waren dabei sogar zum Teil stärker als es statistisch für einen rein additiven Effekt zu erwarten gewesen wäre.

Im Anschluss wurden die Ergebnisse mithilfe des Echtzeit-messenden Zell-Proliferations-Assays *xCELLigence* bestätigt und hinsichtlich des gesamten Behandlungszeitraumes genauer analysiert. Die Viruswachstumskurven zeigten keinen statistisch signifikanten Unterschied, unabhängig davon, ob die humanen Pankreaskarzinomzellen zusätzlich mit Resminostat behandelt worden waren oder nicht.

Weiterhin konnte gezeigt werden, dass der Surrogat-Parameter *zinc-finger-protein 64* (zfp64) nach Resminostatbehandlung sowohl

in unifizierten wie infizierten Pankreaskarzinomzellen vermindert exprimiert wurde, womit die uneingeschränkte pharmakodynamische Funktion bewiesen werden konnte.

Ein Effekt von HDACi, der als grundlegend für den epivirotherapeutischen Ansatz eingestuft wird, besteht in der Hemmung viraler Abwehrmechanismen der Tumorzellen (v.a. IFN-induziert). Im Gegensatz dazu zeigten die Untersuchungen des JAK-STAT-Signalweges (exemplarisch ermittelt durch den Nachweis der Phosphorylierung von STAT1 und der Expression von IFIT1), dass in den infizierten humanen Panreaskarzinomzellen keine Resminostat-basierte Modulation der IFN-Antwort stattfand.

Zusammenfassend kann angenommen werden, dass die beiden Kombinationspartner überwiegend unabhängig voneinander wirken. In einem nächsten Schritt gilt es nun, diese Wirkmechanismen in vivo zu untersuchen und darüber hinaus weiter an der Aufklärung der zugrundeliegenden Mechanismen der epivirotherapeutischen Effizienzverstärkung zu arbeiten.

7. Appendix

7.1. List of figures

7.2. List of tables

7.3. List of abbreviations

5-FU	5-fluorouracil
ANOVA	analysis of variance
APC	antigen-presenting cells
APS	ammonium persulfate
BSA	bovine serum albumin
CAR	coxsackie- and adenovirus receptor
CD	Cluster of differentiation
CDV	canine distemper virus
CPE	cytopathic effect
CSF	colony-stimulating factor
CTCL	cutaneous T-cell lymphoma
CTLA-4	cytotoxic T-lymphocyte-associated protein 4
DC	dendritic cell
ddH2O	double-distilled water
DMEM	Dulbecco’s modified eagle’s medium
DMSO	dimethylsulfoxide
DNA	deoxyribonucleic acid
DSMZ	german collection of microorganisms and cell cultures
ECACC	european collection of authenticated cell cultures
ECM	extracellular matrix
EDTA	ethylenediaminetetraacetic acid
EGFR-TKI	epidermal growth factor receptor tyrosine kinase inhibitor

ELISA	enzyme-linked immunosorbent assay
FCS	fetal calf serum
FDA	food and drug administration
GFP	green fluorescent protein
GM-CSF	Granulocyte-macrophage colony-stimulating factor
GTP	guanosine triphosphate
HAT	histone acyltransferase
HCAC	histone deacetylase
HCC	hepatocellular carcinoma
HIF	hypoxia-inducible factor
hpi	hours post infection
hpt	hours post treatment
HSV	Herpes simplex virus
IFIT1	interferon-induced protein with tetratricopeptide repeats 1
IFN	interferon
IRF	interferon regulatory factor
ISG	interferon-stimulated-gene
KDAC	lysine deacetylase
MeV	measles virus
MHC	major histocompatibility complex
MMP	matrix metalloproteinase
MOI	multiplicity of infection
NF-κB	nuclear factor kappa-light-chain-enhancer of activated B cells
NIS	sodium/iodide symporter

NK	natural killer (cell)
OV	oncolytic virus
PAMP	pathogen-associated molecular patterns
PBS	phosphate buffered saline
PCR	polymerase chain reaction
PDAC	pancreatic ductal adenocarcinoma
PDAC	protein deacetylase
PD-L1	Programmed death-ligand 1
PFU	plaque-forming unit
PVDF	polyvinylidene difluoride
PRR	pattern-recognition-receptor
PSCA	prostate stem cell antigen
PTCL	peripheral T-cell lymphoma
RIG-I	retinoic acid inducible gene I
RNA	ribonucleic acid
ROS	reactive oxygen species
RPV	rinderpest virus
SCD	super cytosine deaminase
SDS	sodium dodecyl sulfate
SLAM	signaling lymphocyte activation molecule
SRB	sulforhodamine B
STAT	signal transducer and activator of transcription
TAA	tumor associated antigen
TCA	trichloroacetic acid
TCID	tissue culture infective dose

TEMED	tetramethylethylenediamine
TRAIL	tumor necrosis factor related apoptosis inducing ligand
TRIS	Tris(hydroxymethyl)aminomethane
VEGF	vascular endothelial growth factor
VPA	valproate

8. References

ABEND, A. & KEHAT, I. 2015. Histone deacetylases as therapeutic targets--from cancer to cardiac disease. *Pharmacol Ther,* 147**,** 55-62.

ACEA BIOSCIENCES, I. 2013. The xCELLigenece system. *ACEA Biosciences, Inc.* San Diego.

ALVAREZ-BRECKENRIDGE, C. A., YU, J., PRICE, R., WEI, M., WANG, Y., NOWICKI, M. O., HA, Y. P., BERGIN, S., HWANG, C., FERNANDEZ, S. A., KAUR, B., CALIGIURI, M. A. & CHIOCCA, E. A. 2012. The histone deacetylase inhibitor valproic acid lessens NK cell action against oncolytic virus-infected glioblastoma cells by inhibition of STAT5/T-BET signaling and generation of gamma interferon. *J Virol,* 86**,** 4566-77.

ANDERSON, B. D., NAKAMURA, T., RUSSELL, S. J. & PENG, K. W. 2004. High CD46 receptor density determines preferential killing of tumor cells by oncolytic measles virus. *Cancer Res,* 64**,** 4919-26.

BERCHTOLD, S., LAMPE, J., WEILAND, T., SMIRNOW, I., SCHLEICHER, S., HANDGRETINGER, R., KOPP, H. G., REISER, J., STUBENRAUCH, F., MAYER, N., MALEK, N. P., BITZER, M. & LAUER, U. M. 2013. Innate immune defense defines susceptibility of sarcoma cells to measles vaccine virus-based oncolysis. *J Virol,* 87**,** 3484-501.

BLUMING, A. Z. & ZIEGLER, J. L. 1971. Regression of Burkitt's lymphoma in association with measles infection. *Lancet,* 2**,** 105-6.

BOFFA, L. C., VIDALI, G., MANN, R. S. & ALLFREY, V. G. 1978. Suppression of histone deacetylation in vivo and in vitro by sodium butyrate. *J Biol Chem,* 253**,** 3364-6.

BOLDEN, J. E., PEART, M. J. & JOHNSTONE, R. W. 2006. Anticancer activities of histone deacetylase inhibitors. *Nat Rev Drug Discov,* 5**,** 769-84.

BOSSOW, S., GROSSARDT, C., TEMME, A., LEBER, M. F., SAWALL, S., RIEBER, E. P., CATTANEO, R., VON KALLE, C. & UNGERECHTS, G. 2011. Armed and targeted measles virus for chemovirotherapy of pancreatic cancer. *Cancer Gene Ther,* 18**,** 598-608.

BOURKE, M. G., SALWA, S., HARRINGTON, K. J., KUCHARCZYK, M. J., FORDE, P. F., DE KRUIJF, M., SODEN, D., TANGNEY, M., COLLINS, J. K. & O'SULLIVAN, G. C. 2011. The emerging role of viruses in the treatment of solid tumours. *Cancer Treat Rev,* 37**,** 618-32.

BRADFORD, M. M. 1976. A rapid and sensitive method for the quantitation of microgram quantities of protein utilizing the principle of protein-dye binding. *Anal Biochem,* 72**,** 248-54.

BREITBACH, C. J., DE SILVA, N. S., FALLS, T. J., ALADL, U., EVGIN, L., PATERSON, J., SUN, Y. Y., ROY, D. G., RINTOUL, J. L., DANESHMAND, M., PARATO, K., STANFORD, M. M., LICHTY, B. D., FENSTER, A., KIRN, D., ATKINS, H. & BELL, J. C. 2011. Targeting tumor vasculature with an oncolytic virus. *Mol Ther,* 19**,** 886-94.

BREITBACH, C. J., PATERSON, J. M., LEMAY, C. G., FALLS, T. J., MCGUIRE, A., PARATO, K. A., STOJDL, D. F., DANESHMAND, M., SPETH, K., KIRN, D., MCCART, J. A., ATKINS, H. & BELL, J. C. 2007. Targeted inflammation during oncolytic virus therapy severely compromises tumor blood flow. *Mol Ther,* 15**,** 1686-93.

BRIDLE, B. W., CHEN, L., LEMAY, C. G., DIALLO, J. S., POL, J., NGUYEN, A., CAPRETTA, A., HE, R., BRAMSON, J. L., BELL, J. C., LICHTY, B. D. & WAN, Y. 2013. HDAC inhibition suppresses primary immune responses, enhances secondary immune responses, and abrogates autoimmunity during tumor immunotherapy. *Mol Ther,* 21**,** 887-94.

BRUNETTO, A. T., ANG, J. E., LAL, R., OLMOS, D., MOLIFE, L. R., KRISTELEIT, R., PARKER, A., CASAMAYOR, I., OLALEYE, M., MAIS, A., HAUNS, B., STROBEL, V., HENTSCH, B. & DE BONO, J. S. 2013. First-in-human, pharmacokinetic and pharmacodynamic phase I study of Resminostat, an oral histone deacetylase inhibitor, in patients with advanced solid tumors. *Clin Cancer Res,* 19**,** 5494-504.

BUCHWALD, M., KRAMER, O. H. & HEINZEL, T. 2009. HDACi--targets beyond chromatin. *Cancer Lett,* 280**,** 160-7.

BURRIS, H. A., 3RD, MOORE, M. J., ANDERSEN, J., GREEN, M. R., ROTHENBERG, M. L., MODIANO, M. R., CRIPPS, M. C., PORTENOY, R. K., STORNIOLO, A. M., TARASSOFF, P., NELSON, R., DORR, F. A., STEPHENS, C. D. & VON HOFF, D. D.

1997. Improvements in survival and clinical benefit with gemcitabine as first-line therapy for patients with advanced pancreas cancer: a randomized trial. *J Clin Oncol,* 15**,** 2403-13.

CHANG, H. M., PAULSON, M., HOLKO, M., RICE, C. M., WILLIAMS, B. R., MARIE, I. & LEVY, D. E. 2004. Induction of interferon-stimulated gene expression and antiviral responses require protein deacetylase activity. *Proc Natl Acad Sci U S A,* 101**,** 9578-83.

CHIOCCA, E. A. 2008. The host response to cancer virotherapy. *Curr Opin Mol Ther,* 10**,** 38-45.

COFFIN, R. S. 2015. From virotherapy to oncolytic immunotherapy: where are we now? *Curr Opin Virol,* 13**,** 93-100.

CONROY, T., DESSEIGNE, F., YCHOU, M., BOUCHE, O., GUIMBAUD, R., BECOUARN, Y., ADENIS, A., RAOUL, J. L., GOURGOU-BOURGADE, S., DE LA FOUCHARDIERE, C., BENNOUNA, J., BACHET, J. B., KHEMISSA-AKOUZ, F., PERE-VERGE, D., DELBALDO, C., ASSENAT, E., CHAUFFERT, B., MICHEL, P., MONTOTO-GRILLOT, C., DUCREUX, M., GROUPE TUMEURS DIGESTIVES OF, U. & INTERGROUP, P. 2011. FOLFIRINOX versus gemcitabine for metastatic pancreatic cancer. *N Engl J Med,* 364**,** 1817-25.

CRIPE, T. P., WANG, P. Y., MARCATO, P., MAHLLER, Y. Y. & LEE, P. W. 2009. Targeting cancer-initiating cells with oncolytic viruses. *Mol Ther,* 17**,** 1677-82.

DERYUGINA, E. I. & QUIGLEY, J. P. 2015. Tumor angiogenesis: MMP-mediated induction of intravasation- and metastasis-sustaining neovasculature. *Matrix Biol*.

DIAMOND, M. S. & FARZAN, M. 2013. The broad-spectrum antiviral functions of IFIT and IFITM proteins. *Nat Rev Immunol,* 13**,** 46-57.

DOKMANOVIC, M., CLARKE, C. & MARKS, P. A. 2007. Histone deacetylase inhibitors: overview and perspectives. *Mol Cancer Res,* 5**,** 981-9.

DREUX, M. & CHISARI, F. V. 2010. Viruses and the autophagy machinery. *Cell Cycle,* 9**,** 1295-1307.

DUPREX, W. P., MCQUAID, S., HANGARTNER, L., BILLETER, M. A. & RIMA, B. K. 1999. Observation of measles virus cell-to-cell spread in astrocytoma cells by using a green fluorescent protein-expressing recombinant virus. *J Virol,* 73**,** 9568-75.

DUPREX, W. P. & RIMA, B. K. 2002. Using green fluorescent protein to monitor measles virus cell-to-cell spread by time-lapse confocal microscopy. *Methods Mol Biol,* 183**,** 297-307.

ELLERHOFF, T. P., BERCHTOLD, S., VENTURELLI, S., BURKARD, M., SMIRNOW, I., WULFF, T. & LAUER, U. M. 2016. Novel epi-virotherapeutic treatment of pancreatic cancer combining the oral histone deacetylase inhibitor resminostat with oncolytic measles vaccine virus. *Int J Oncol*.

ENGELAND, C. E., GROSSARDT, C., VEINALDE, R., BOSSOW, S., LUTZ, D., KAUFMANN, J. K., SHEVCHENKO, I., UMANSKY, V., NETTELBECK, D. M., WEICHERT, W., JAGER, D., VON KALLE, C. & UNGERECHTS, G. 2014. CTLA-4 and PD-L1 checkpoint blockade enhances oncolytic measles virus therapy. *Mol Ther,* 22**,** 1949-59.

ESCOBAR-ZARATE, D., LIU, Y. P., SUKSANPAISAN, L., RUSSELL, S. J. & PENG, K. W. 2013. Overcoming cancer cell resistance to VSV oncolysis with JAK1/2 inhibitors. *Cancer Gene Ther,* 20**,** 582-9.

FENG, W., ZHANG, B., CAI, D. & ZOU, X. 2014. Therapeutic potential of histone deacetylase inhibitors in pancreatic cancer. *Cancer Lett,* 347**,** 183-90.

FILLAT, C., MALIANDI, M. V., MATO-BERCIANO, A. & ALEMANY, R. 2014. Combining oncolytic virotherapy and cytotoxic therapies to fight cancer. *Curr Pharm Des,* 20**,** 6513-21.

FISHELSON, Z., DONIN, N., ZELL, S., SCHULTZ, S. & KIRSCHFINK, M. 2003. Obstacles to cancer immunotherapy: expression of membrane complement regulatory proteins (mCRPs) in tumors. *Mol Immunol,* 40**,** 109-23.

FRAGA, M. F., BALLESTAR, E., VILLAR-GAREA, A., BOIX-CHORNET, M., ESPADA, J., SCHOTTA, G., BONALDI, T., HAYDON, C., ROPERO, S., PETRIE, K., IYER, N. G., PEREZ-ROSADO, A., CALVO, E., LOPEZ, J. A., CANO, A., CALASANZ, M. J., COLOMER, D., PIRIS, M. A., AHN, N., IMHOF, A., CALDAS, C., JENUWEIN, T. & ESTELLER, M. 2005. Loss of acetylation at Lys16 and trimethylation at Lys20 of histone H4 is a common hallmark of human cancer. *Nat Genet,* 37**,** 391-400.

FRIDMAN, W. H., PAGÈS, F., SAUTÈS-FRIDMAN, C. & GALON, J. 2012. The immune contexture in human tumours: impact on clinical outcome. *Nat Rev Cancer,* 12**,** 298-306.

FUERTES, M. B., KACHA, A. K., KLINE, J., WOO, S. R., KRANZ, D. M., MURPHY, K. M. & GAJEWSKI, T. F. 2011. Host type I IFN signals are required for antitumor CD8+ T cell responses through CD8{alpha}+ dendritic cells. *J Exp Med,* 208**,** 2005-16.

GALON, J., PAGES, F., MARINCOLA, F. M., ANGELL, H. K., THURIN, M., LUGLI, A., ZLOBEC, I., BERGER, A., BIFULCO, C., BOTTI, G., TATANGELO, F., BRITTEN, C. M., KREITER, S., CHOUCHANE, L., DELRIO, P., ARNDT, H., ASSLABER, M., MAIO, M., MASUCCI, G. V., MIHM, M., VIDAL-VANACLOCHA, F., ALLISON, J. P., GNJATIC, S., HAKANSSON, L., HUBER, C., SINGH-JASUJA, H., OTTENSMEIER, C., ZWIERZINA, H., LAGHI, L., GRIZZI, F., OHASHI, P. S., SHAW, P. A., CLARKE, B. A., WOUTERS, B. G., KAWAKAMI, Y., HAZAMA, S., OKUNO, K., WANG, E., O'DONNELL-TORMEY, J., LAGORCE, C., PAWELEC, G., NISHIMURA, M. I., HAWKINS, R., LAPOINTE, R., LUNDQVIST, A., KHLEIF, S. N., OGINO, S., GIBBS, P., WARING, P., SATO, N., TORIGOE, T., ITOH, K., PATEL, P. S., SHUKLA, S. N., PALMQVIST, R., NAGTEGAAL, I. D., WANG, Y., D'ARRIGO, C., KOPETZ, S., SINICROPE, F. A., TRINCHIERI, G., GAJEWSKI, T. F., ASCIERTO, P. A. & FOX, B. A. 2012. Cancer classification using the Immunoscore: a worldwide task force. *J Transl Med,* 10**,** 205.

GAMMOH, N., LAM, D., PUENTE, C., GANLEY, I., MARKS, P. A. & JIANG, X. 2012. Role of autophagy in histone deacetylase inhibitor-induced apoptotic and nonapoptotic cell death. *Proc Natl Acad Sci U S A,* 109**,** 6561-5.

GARRIDO-LAGUNA, I. & HIDALGO, M. 2015. Pancreatic cancer: from state-of-the-art treatments to promising novel therapies. *Nat Rev Clin Oncol*.

GENIN, P., MORIN, P. & CIVAS, A. 2003. Impairment of interferon-induced IRF-7 gene expression due to inhibition of ISGF3 formation by trichostatin A. *J Virol,* 77**,** 7113-9.

GIORDA, K. M. & HEBERT, D. N. 2013. Viroporins customize host cells for efficient viral propagation. *DNA Cell Biol,* 32**,** 557-64.

GLOZAK, M. A., SENGUPTA, N., ZHANG, X. & SETO, E. 2005. Acetylation and deacetylation of non-histone proteins. *Gene,* 363**,** 15-23.

GLOZAK, M. A. & SETO, E. 2007. Histone deacetylases and cancer. *Oncogene,* 26**,** 5420-32.

GROSSARDT, C., ENGELAND, C. E., BOSSOW, S., HALAMA, N., ZAOUI, K., LEBER, M. F., SPRINGFELD, C., JAEGER, D., VON KALLE, C. & UNGERECHTS, G. 2013. Granulocyte-macrophage colony-stimulating factor-armed oncolytic measles virus is an effective therapeutic cancer vaccine. *Hum Gene Ther,* 24**,** 644-54.

GUILLERME, J. B., GREGOIRE, M., TANGY, F. & FONTENEAU, J. F. 2013. Antitumor Virotherapy by Attenuated Measles Virus (MV). *Biology (Basel),* 2**,** 587-602.

GUJAR, S., DIELSCHNEIDER, R., CLEMENTS, D., HELSON, E., SHMULEVITZ, M., MARCATO, P., PAN, D., PAN, L. Z., AHN, D. G., ALAWADHI, A. & LEE, P. W. 2013. Multifaceted therapeutic targeting of ovarian peritoneal carcinomatosis through virus-induced immunomodulation. *Mol Ther,* 21**,** 338-47.

HALL, J. C. & ROSEN, A. 2010. Type I interferons: crucial participants in disease amplification in autoimmunity. *Nat Rev Rheumatol,* 6**,** 40-9.

HAMMILL, A. M., CONNER, J. & CRIPE, T. P. 2010. Oncolytic virotherapy reaches adolescence. *Pediatr Blood Cancer,* 55**,** 1253-63.

HARALAMBIEVA, I., IANKOV, I., HASEGAWA, K., HARVEY, M., RUSSELL, S. J. & PENG, K. W. 2007. Engineering oncolytic measles virus to circumvent the intracellular innate immune response. *Mol Ther,* 15**,** 588-97.

HAVIV, Y. S., BLACKWELL, J. L., KANERVA, A., NAGI, P., KRASNYKH, V., DMITRIEV, I., WANG, M., NAITO, S., LEI, X., HEMMINKI, A., CAREY, D. & CURIEL, D. T. 2002. Adenoviral gene therapy for renal cancer requires retargeting to alternative cellular receptors. *Cancer Res,* 62**,** 4273-81.

HEINZERLING, L., KUNZI, V., OBERHOLZER, P. A., KUNDIG, T., NAIM, H. & DUMMER, R. 2005. Oncolytic measles virus in cutaneous T-cell lymphomas mounts antitumor immune responses in vivo and targets interferon-resistant tumor cells. *Blood,* 106**,** 2287-94.

HIDALGO, M. 2010. Pancreatic cancer. *N Engl J Med,* 362**,** 1605-17.

HONDA, K., TAKAOKA, A. & TANIGUCHI, T. 2006. Type I interferon [corrected] gene induction by the interferon regulatory factor family of transcription factors. *Immunity,* 25**,** 349-60.

HRISTOV, G., KRAMER, M., LI, J., EL-ANDALOUSSI, N., MORA, R., DAEFFLER, L., ZENTGRAF, H., ROMMELAERE, J. & MARCHINI, A. 2010. Through its nonstructural protein NS1, parvovirus H-1 induces apoptosis via accumulation of reactive oxygen species. *J Virol,* 84**,** 5909-22.

HUSZTHY, P. C., IMMERVOLL, H., WANG, J., GOPLEN, D., MILETIC, H., EIDE, G. E. & BJERKVIG, R. 2010. Cellular effects of oncolytic viral therapy on the glioblastoma microenvironment. *Gene Ther,* 17**,** 202-16.

HUTZEN B, R. C., STUDEBAKER AW 2015. Advances in the design and development of oncolytic measles viruses. *Dovepress,* 2015:4**,** 109—118.

KADOTA, S. & NAGATA, K. 2011. pp32, an INHAT component, is a transcription machinery recruiter for maximal induction of IFN-stimulated genes. *J Cell Sci,* 124**,** 892-9.

KARBER, G. 1931. "Beitrag zur kollektiven Behandlung pharmakologischer Reihenversuch. *Archiv fur Experimentelle Pathologie und Pharmakologie,* 162.

KASMAN, L., ONICESCU, G. & VOELKEL-JOHNSON, C. 2012. Histone deacetylase inhibitors restore cell surface expression of the coxsackie adenovirus receptor and enhance CMV promoter activity in castration-resistant prostate cancer cells. *Prostate Cancer,* 2012**,** 137163.

KATSURA, T., IWAI, S., OTA, Y., SHIMIZU, H., IKUTA, K. & YURA, Y. 2009. The effects of trichostatin A on the oncolytic ability of herpes simplex virus for oral squamous cell carcinoma cells. *Cancer Gene Ther,* 16**,** 237-45.

KAUFMAN, H. L., KOHLHAPP, F. J. & ZLOZA, A. 2015. Oncolytic viruses: a new class of immunotherapy drugs. *Nat Rev Drug Discov,* 14**,** 642-62.

KAWAGUCHI, Y., KOVACS, J. J., MCLAURIN, A., VANCE, J. M., ITO, A. & YAO, T. P. 2003. The deacetylase HDAC6 regulates aggresome formation and cell viability in response to misfolded protein stress. *Cell,* 115**,** 727-38.

KELLY, E. & RUSSELL, S. J. 2007. History of oncolytic viruses: genesis to genetic engineering. *Mol Ther,* 15**,** 651-9.

KHAN, O. & LA THANGUE, N. B. 2012. HDAC inhibitors in cancer biology: emerging mechanisms and clinical applications. *Immunol Cell Biol,* 90**,** 85-94.

KIM, M., ZINN, K. R., BARNETT, B. G., SUMEREL, L. A., KRASNYKH, V., CURIEL, D. T. & DOUGLAS, J. T. 2002. The therapeutic efficacy of adenoviral vectors for cancer gene therapy is limited by a low level of primary adenovirus receptors on tumour cells. *Eur J Cancer,* 38**,** 1917-26.

KINDLER, H. L., NIEDZWIECKI, D., HOLLIS, D., SUTHERLAND, S., SCHRAG, D., HURWITZ, H., INNOCENTI, F., MULCAHY, M. F., O'REILLY, E., WOZNIAK, T. F., PICUS, J., BHARGAVA, P., MAYER, R. J., SCHILSKY, R. L. & GOLDBERG, R. M. 2010. Gemcitabine plus bevacizumab compared with gemcitabine plus placebo in patients with advanced pancreatic cancer: phase III trial of the Cancer and Leukemia Group B (CALGB 80303). *J Clin Oncol,* 28**,** 3617-22.

KOUTSOUNAS, I., GIAGINIS, C. & THEOCHARIS, S. 2013. Histone deacetylase inhibitors and pancreatic cancer: are there any promising clinical trials? *World J Gastroenterol,* 19**,** 1173-81.

KOUZARIDES, T. 2007. Chromatin modifications and their function. *Cell,* 128**,** 693-705.

KROESEN, M., GIELEN, P., BROK, I. C., ARMANDARI, I., HOOGERBRUGGE, P. M. & ADEMA, G. J. 2014. HDAC inhibitors and immunotherapy; a double edged sword? *Oncotarget,* 5**,** 6558-72.

LAEMMLI, U. K. 1970. Cleavage of structural proteins during the assembly of the head of bacteriophage T4. *Nature,* 227**,** 680-5.

LAMPE, J., BOSSOW, S., WEILAND, T., SMIRNOW, I., LEHMANN, R., NEUBERT, W., BITZER, M. & LAUER, U. M. 2013. An armed oncolytic measles vaccine virus eliminates human hepatoma cells independently of apoptosis. *Gene Ther,* 20**,** 1033-41.

LEDFORD, H. 2015. Cancer-fighting viruses win approval. *Nature,* 526**,** 622-3.

LETTIERI, C. K., HINGORANI, P. & KOLB, E. A. 2012. Progress of oncolytic viruses in sarcomas. *Expert Rev Anticancer Ther,* 12**,** 229-42.

LI, D., DUAN, L., FREIMUTH, P. & O'MALLEY, B. W., JR. 1999. Variability of adenovirus receptor density influences gene transfer efficiency and therapeutic response in head and neck cancer. *Clin Cancer Res,* 5**,** 4175-81.

LI, J., BONIFATI, S., HRISTOV, G., MARTTILA, T., VALMARY-DEGANO, S., STANZEL, S., SCHNOLZER, M., MOUGIN, C., APRAHAMIAN, M., GREKOVA, S. P., RAYKOV, Z., ROMMELAERE, J. & MARCHINI, A. 2013. Synergistic combination of valproic acid and oncolytic parvovirus H-1PV as a potential therapy against cervical and pancreatic carcinomas. *EMBO Mol Med,* 5**,** 1537-55.

LICHTY, B. D., BREITBACH, C. J., STOJDL, D. F. & BELL, J. C. 2014. Going viral with cancer immunotherapy. *Nat Rev Cancer,* 14**,** 559-67.

LIEVANO, F., GALEA, S. A., THORNTON, M., WIEDMANN, R. T., MANOFF, S. B., TRAN, T. N., AMIN, M. A., SEMINACK, M. M., VAGIE, K. A., DANA, A. & PLOTKIN, S. A. 2012. Measles, mumps, and rubella virus vaccine (M-M-RII): a review of 32 years of clinical and postmarketing experience. *Vaccine,* 30**,** 6918-26.

LIU, T. C., CASTELO-BRANCO, P., RABKIN, S. D. & MARTUZA, R. L. 2008. Trichostatin A and oncolytic HSV combination therapy shows enhanced antitumoral and antiangiogenic effects. *Mol Ther,* 16**,** 1041-7.

LIU, T. C., GALANIS, E. & KIRN, D. 2007. Clinical trial results with oncolytic virotherapy: a century of promise, a decade of progress. *Nat Clin Pract Oncol,* 4**,** 101-17.

LONG, J., ZHANG, Y., YU, X., YANG, J., LEBRUN, D. G., CHEN, C., YAO, Q. & LI, M. 2011. Overcoming drug resistance in pancreatic cancer. *Expert Opin Ther Targets,* 15**,** 817-28.

MA, J., ZHAO, J., LU, J., JIANG, Y., YANG, H., LI, P., ZHAO, M., LIU, K. & DONG, Z. 2012. Coxsackievirus and adenovirus receptor promotes antitumor activity of oncolytic adenovirus H101 in esophageal cancer. *Int J Mol Med,* 30**,** 1403-9.

MACTAVISH, H., DIALLO, J. S., HUANG, B., STANFORD, M., LE BOEUF, F., DE SILVA, N., COX, J., SIMMONS, J. G., GUIMOND, T., FALLS, T., MCCART, J. A., ATKINS, H., BREITBACH, C., KIRN, D., THORNE, S. & BELL, J. C. 2010. Enhancement of vaccinia virus based oncolysis with histone deacetylase inhibitors. *PLoS One,* 5**,** e14462.

MAISONNEUVE, P. & LOWENFELS, A. B. 2015. Risk factors for pancreatic cancer: a summary review of meta-analytical studies. *Int J Epidemiol,* 44**,** 186-98.

MANDL-WEBER, S., MEINEL, F. G., JANKOWSKY, R., ODUNCU, F., SCHMIDMAIER, R. & BAUMANN, P. 2010. The novel inhibitor of histone deacetylase resminostat (RAS2410) inhibits proliferation and induces apoptosis in multiple myeloma (MM) cells. *Br J Haematol,* 149**,** 518-28.

MELCHER, A., PARATO, K., ROONEY, C. M. & BELL, J. C. 2011. Thunder and lightning: immunotherapy and oncolytic viruses collide. *Mol Ther,* 19**,** 1008-16.

MENG, S., XU, J., WU, Y. & DING, C. 2013. Targeting autophagy to enhance oncolytic virus-based cancer therapy. *Expert Opin Biol Ther,* 13**,** 863-73.

MIYAMOTO, H., MURAKAMI, T., TSUCHIDA, K., SUGINO, H., MIYAKE, H. & TASHIRO, S. 2004. Tumor-stroma interaction of human pancreatic cancer: acquired resistance to anticancer drugs and proliferation regulation is dependent on extracellular matrix proteins. *Pancreas,* 28**,** 38-44.

MOEHLER, M. H., ZEIDLER, M., WILSBERG, V., CORNELIS, J. J., WOELFEL, T., ROMMELAERE, J., GALLE, P. R. & HEIKE, M. 2005. Parvovirus H-1-induced tumor cell death enhances human immune response in vitro via increased phagocytosis, maturation, and cross-presentation by dendritic cells. *Hum Gene Ther,* 16**,** 996-1005.

MOHAMMED, S., VAN BUREN, G., 2ND & FISHER, W. E. 2014. Pancreatic cancer: advances in treatment. *World J Gastroenterol,* 20**,** 9354-60.

MOORE, A. E. 1954. Effects of viruses on tumors. *Annu Rev Microbiol,* 8**,** 393-410.

MORETTA, L., BOTTINO, C., PENDE, D., VITALE, M., MINGARI, M. C. & MORETTA, A. 2005. Human natural killer cells: Molecular mechanisms controlling NK cell activation and tumor cell lysis. *Immunol Lett,* 100**,** 7-13.

MOSS, W. J. & GRIFFIN, D. E. 2006. Global measles elimination. *Nat Rev Microbiol,* 4**,** 900-8.

MOTTAMAL, M., ZHENG, S., HUANG, T. L. & WANG, G. 2015. Histone Deacetylase Inhibitors in Clinical Studies as Templates for New Anticancer Agents. *Molecules,* 20**,** 3898-3941.

MSAOUEL, P., IANKOV, I. D., DISPENZIERI, A. & GALANIS, E. 2012. Attenuated oncolytic measles virus strains as cancer therapeutics. *Curr Pharm Biotechnol,* 13**,** 1732-41.

MSAOUEL, P., OPYRCHAL, M., DOMINGO MUSIBAY, E. & GALANIS, E. 2013. Oncolytic measles virus strains as novel anticancer agents. *Expert Opin Biol Ther,* 13**,** 483-502.

MURROW, L. & DEBNATH, J. 2013. Autophagy as a stress-response and quality-control mechanism: implications for cell injury and human disease. *Annu Rev Pathol,* 8**,** 105-37.

NAKASHIMA, H., KAUFMANN, J. K., WANG, P. Y., NGUYEN, T., SPERANZA, M. C., KASAI, K., OKEMOTO, K., OTSUKI, A., NAKANO, I., FERNANDEZ, S., GOINS, W. F., GRANDI, P., GLORIOSO, J. C., LAWLER, S., CRIPE, T. P. & CHIOCCA, E. A. 2015a. Histone deacetylase 6 inhibition enhances oncolytic viral replication in glioma. *J Clin Invest,* 125**,** 4269-80.

NAKASHIMA, H., NGUYEN, T. & CHIOCCA, E. A. 2015b. Combining HDAC inhibitors with oncolytic virotherapy for cancer therapy. *Dovepress,* 2015:4**,** 183-191.

NGUYEN, T. L., ABDELBARY, H., ARGUELLO, M., BREITBACH, C., LEVEILLE, S., DIALLO, J. S., YASMEEN, A., BISMAR, T. A., KIRN, D., FALLS, T., SNOULTEN, V. E., VANDERHYDEN, B. C., WERIER, J., ATKINS, H., VAHA-KOSKELA, M. J., STOJDL, D. F., BELL, J. C. & HISCOTT, J. 2008. Chemical targeting of the innate antiviral response by histone deacetylase inhibitors renders refractory cancers sensitive to viral oncolysis. *Proc Natl Acad Sci U S A,* 105**,** 14981-6.

NGUYEN, T. L., WILSON, M. G. & HISCOTT, J. 2010. Oncolytic viruses and histone deacetylase inhibitors--a multi-pronged strategy to target tumor cells. *Cytokine Growth Factor Rev,* 21**,** 153-9.

NIELSEN, L., BLIXENKRONE-MOLLER, M., THYLSTRUP, M., HANSEN, N. J. & BOLT, G. 2001. Adaptation of wild-type measles virus to CD46 receptor usage. *Arch Virol,* 146**,** 197-208.

NUSINZON, I. & HORVATH, C. M. 2006. Positive and negative regulation of the innate antiviral response and beta interferon gene expression by deacetylation. *Mol Cell Biol,* 26**,** 3106-13.

OGBOMO, H., MICHAELIS, M., KREUTER, J., DOERR, H. W. & CINATL, J., JR. 2007. Histone deacetylase inhibitors suppress natural killer cell cytolytic activity. *FEBS Lett,* 581**,** 1317-22.

OTSUKI, A., PATEL, A., KASAI, K., SUZUKI, M., KUROZUMI, K., CHIOCCA, E. A. & SAEKI, Y. 2008. Histone deacetylase inhibitors augment antitumor efficacy of herpes-based oncolytic viruses. *Mol Ther,* 16**,** 1546-55.

PARK, J., THOMAS, S. & MUNSTER, P. N. 2015. Epigenetic modulation with histone deacetylase inhibitors in combination with immunotherapy. *Epigenomics,* 7**,** 641-52.

POL, J., BLOY, N., OBRIST, F., EGGERMONT, A., GALON, J., CREMER, I., ERBS, P., LIMACHER, J. M., PREVILLE, X., ZITVOGEL, L., KROEMER, G. & GALLUZZI, L. 2014. Trial Watch:: Oncolytic viruses for cancer therapy. *Oncoimmunology,* 3**,** e28694.

POLEVODA, B. & SHERMAN, F. 2000. Nalpha -terminal acetylation of eukaryotic proteins. *J Biol Chem,* 275**,** 36479-82.

POLEVODA, B. & SHERMAN, F. 2002. The diversity of acetylated proteins. *Genome Biol,* 3**,** reviews0006.

PRESTWICH, R. J., ERRINGTON, F., DIAZ, R. M., PANDHA, H. S., HARRINGTON, K. J., MELCHER, A. A. & VILE, R. G. 2009. The case of oncolytic viruses versus the immune system: waiting on the judgment of Solomon. *Hum Gene Ther,* 20**,** 1119-32.

RAJENDRAN, P., WILLIAMS, D. E., HO, E. & DASHWOOD, R. H. 2011. Metabolism as a key to histone deacetylase inhibition. *Crit Rev Biochem Mol Biol,* 46**,** 181-99.

RAO, C. V. & MOHAMMED, A. 2015. New insights into pancreatic cancer stem cells. *World J Stem Cells,* 7**,** 547-55.

RICHETTA, C., GREGOIRE, I. P., VERLHAC, P., AZOCAR, O., BAGUET, J., FLACHER, M., TANGY, F., RABOURDIN-COMBE, C. & FAURE, M. 2013. Sustained autophagy contributes to measles virus infectivity. *PLoS Pathog,* 9**,** e1003599.

RIGGS, M. G., WHITTAKER, R. G., NEUMANN, J. R. & INGRAM, V. M. 1977. n-Butyrate causes histone modification in HeLa and Friend erythroleukaemia cells. *Nature,* 268**,** 462-4.

RUF, B., BERCHTOLD, S., VENTURELLI, S., BURKARD, M., SMIRNOW, I., PRENZEL, T., HENNING, S. W. & LAUER, U. M. 2015. Combination of the oral histone deacetylase inhibitor resminostat with oncolytic measles vaccine virus as a new option for epi-

virotherapeutic treatment of hepatocellular carcinoma. *Molecular Therapy — Oncolytics,* 2**,** 15019.
RUSSELL, S. J., FEDERSPIEL, M. J., PENG, K. W., TONG, C., DINGLI, D., MORICE, W. G., LOWE, V., O'CONNOR, M. K., KYLE, R. A., LEUNG, N., BUADI, F. K., RAJKUMAR, S. V., GERTZ, M. A., LACY, M. Q. & DISPENZIERI, A. 2014. Remission of disseminated cancer after systemic oncolytic virotherapy. *Mayo Clin Proc,* 89**,** 926-33.
RUSSELL, S. J. & PENG, K. W. 2009. Measles virus for cancer therapy. *Curr Top Microbiol Immunol,* 330**,** 213-41.
RUSSELL, S. J., PENG, K. W. & BELL, J. C. 2012. Oncolytic virotherapy. *Nat Biotechnol,* 30**,** 658-70.
SACHS, M. D., RAMAMURTHY, M., POEL, H., WICKHAM, T. J., LAMFERS, M., GERRITSEN, W., CHOWDHURY, W., LI, Y., SCHOENBERG, M. P. & RODRIGUEZ, R. 2004. Histone deacetylase inhibitors upregulate expression of the coxsackie adenovirus receptor (CAR) preferentially in bladder cancer cells. *Cancer Gene Ther,* 11**,** 477-86.
SAITO, K., SAKAGUCHI, M., IIOKA, H., MATSUI, M., NAKANISHI, H., HUH, N. H. & KONDO, E. 2014. Coxsackie and adenovirus receptor is a critical regulator for the survival and growth of oral squamous carcinoma cells. *Oncogene,* 33**,** 1274-86.
SATO, H., YONEDA, M., HONDA, T. & KAI, C. 2012. Morbillivirus receptors and tropism: multiple pathways for infection. *Front Microbiol,* 3**,** 75.
SCHNEIDER, G., KRAMER, O. H., FRITSCHE, P., SCHULER, S., SCHMID, R. M. & SAUR, D. 2010. Targeting histone deacetylases in pancreatic ductal adenocarcinoma. *J Cell Mol Med,* 14**,** 1255-63.
SCHNEIDER, W. M., CHEVILLOTTE, M. D. & RICE, C. M. 2014. Interferon-stimulated genes: a complex web of host defenses. *Annu Rev Immunol,* 32**,** 513-45.
SCHOGGINS, J. W. & RICE, C. M. 2011. Interferon-stimulated genes and their antiviral effector functions. *Current opinion in virology,* 1**,** 519-525.
SEALY, L. & CHALKLEY, R. 1978. The effect of sodium butyrate on histone modification. *Cell,* 14**,** 115-21.
SEN, G. C. 2001. Viruses and interferons. *Annu Rev Microbiol,* 55**,** 255-81.
SETIADI, A. F., OMILUSIK, K., DAVID, M. D., SEIPP, R. P., HARTIKAINEN, J., GOPAUL, R., CHOI, K. B. & JEFFERIES, W. A. 2008. Epigenetic enhancement of antigen processing and presentation promotes immune recognition of tumors. *Cancer Res,* 68**,** 9601-7.
SHULAK, L., BELJANSKI, V., CHIANG, C., DUTTA, S. M., VAN GREVENYNGHE, J., BELGNAOUI, S. M., NGUYEN, T. L., DI LENARDO, T., SEMMES, O. J., LIN, R. & HISCOTT, J. 2014. Histone deacetylase inhibitors potentiate vesicular stomatitis virus oncolysis in prostate cancer cells by modulating NF-kappaB-dependent autophagy. *J Virol,* 88**,** 2927-40.
SIEGEL, R., NAISHADHAM, D. & JEMAL, A. 2013. Cancer statistics, 2013. *CA Cancer J Clin,* 63**,** 11-30.
SMITH, T. T., ROTH, J. C., FRIEDMAN, G. K. & GILLESPIE, G. Y. 2014. Oncolytic viral therapy: targeting cancer stem cells. *Oncolytic Virother,* 2014**,** 21-33.
SOUTHAM, C. M. 1960. Present status of oncolytic virus studies. *Trans N Y Acad Sci,* 22**,** 657-73.
SPANGE, S., WAGNER, T., HEINZEL, T. & KRAMER, O. H. 2009. Acetylation of non-histone proteins modulates cellular signalling at multiple levels. *Int J Biochem Cell Biol,* 41**,** 185-98.
SPEARMAN, C. 1908. The Method of 'Right and Wrong' Cases ('Constant Stimuli') Without Gauss's Fonnula. *British Journal of Psychology,* 2.
STEINS, M., THOMAS, M. & GEISSLER, M. 2014. Erlotinib. *Recent Results Cancer Res,* 201**,** 109-23.
STOJDL, D. F., LICHTY, B. D., TENOEVER, B. R., PATERSON, J. M., POWER, A. T., KNOWLES, S., MARIUS, R., REYNARD, J., POLIQUIN, L., ATKINS, H., BROWN, E. G., DURBIN, R. K., DURBIN, J. E., HISCOTT, J. & BELL, J. C. 2003. VSV strains with defects in their ability to shutdown innate immunity are potent systemic anti-cancer agents. *Cancer Cell,* 4**,** 263-75.
SUTTON, J. M. & ABBOTT, D. E. 2014. Neoadjuvant therapy for pancreas cancer: past lessons and future therapies. *World J Gastroenterol,* 20**,** 15564-79.

TAKEUCHI, K., MIYAJIMA, N., NAGATA, N., TAKEDA, M. & TASHIRO, M. 2003. Wild-type measles virus induces large syncytium formation in primary human small airway epithelial cells by a SLAM(CD150)-independent mechanism. *Virus Res,* 94**,** 11-6.

TANAKA, S. 2015. Molecular Pathogenesis and Targeted Therapy of Pancreatic Cancer. *Ann Surg Oncol*.

TANG, X., GAO, J. S., GUAN, Y. J., MCLANE, K. E., YUAN, Z. L., RAMRATNAM, B. & CHIN, Y. E. 2007. Acetylation-dependent signal transduction for type I interferon receptor. *Cell,* 131**,** 93-105.

TAQI, A. M., ABDURRAHMAN, M. B., YAKUBU, A. M. & FLEMING, A. F. 1981. Regression of Hodgkin's disease after measles. *Lancet,* 1**,** 1112.

TEAGUE, A., LIM, K. H. & WANG-GILLAM, A. 2015. Advanced pancreatic adenocarcinoma: a review of current treatment strategies and developing therapies. *Ther Adv Med Oncol,* 7**,** 68-84.

THURN, K. T., THOMAS, S., MOORE, A. & MUNSTER, P. N. 2011. Rational therapeutic combinations with histone deacetylase inhibitors for the treatment of cancer. *Future Oncol,* 7**,** 263-83.

VICHAI, V. & KIRTIKARA, K. 2006. Sulforhodamine B colorimetric assay for cytotoxicity screening. *Nat Protoc,* 1**,** 1112-6.

VLASAKOVA, J., NOVAKOVA, Z., ROSSMEISLOVA, L., KAHLE, M., HOZAK, P. & HODNY, Z. 2007. Histone deacetylase inhibitors suppress IFNalpha-induced up-regulation of promyelocytic leukemia protein. *Blood,* 109**,** 1373-80.

WENNIER, S., LI, S. & MCFADDEN, G. 2011. Oncolytic virotherapy for pancreatic cancer. *Expert Rev Mol Med,* 13**,** e18.

WHITE, E. & DIPAOLA, R. S. 2009. The double-edged sword of autophagy modulation in cancer. *Clin Cancer Res,* 15**,** 5308-16.

WHITE, M. C. & FRAMPTON, A. R., JR. 2013. The histone deacetylase inhibitor valproic acid enhances equine herpesvirus type 1 (EHV-1)-mediated oncolysis of human glioma cells. *Cancer Gene Ther,* 20**,** 88-93.

WHITE, M. K., PAGANO, J. S. & KHALILI, K. 2014. Viruses and human cancers: a long road of discovery of molecular paradigms. *Clin Microbiol Rev,* 27**,** 463-81.

WOLLER, N., GURLEVIK, E., URECHE, C. I., SCHUMACHER, A. & KUHNEL, F. 2014. Oncolytic viruses as anticancer vaccines. *Front Oncol,* 4**,** 188.

WOLLMANN, G., OZDUMAN, K. & VAN DEN POL, A. N. 2012. Oncolytic virus therapy for glioblastoma multiforme: concepts and candidates. *Cancer J,* 18**,** 69-81.

WUNDER, T., SCHMID, K., WICKLEIN, D., GROITL, P., DOBNER, T., LANGE, T., ANDERS, M. & SCHUMACHER, U. 2013. Expression of the coxsackie adenovirus receptor in neuroendocrine lung cancers and its implications for oncolytic adenoviral infection. *Cancer Gene Ther,* 20**,** 25-32.

XU, C., LI, H., SU, C. & LI, Z. 2013. Viral therapy for pancreatic cancer: tackle the bad guys with poison. *Cancer Lett,* 333**,** 1-8.

YANAGI, Y., TAKEDA, M. & OHNO, S. 2006. Measles virus: cellular receptors, tropism and pathogenesis. *J Gen Virol,* 87**,** 2767-79.

YANG, S., WANG, X., CONTINO, G., LIESA, M., SAHIN, E., YING, H., BAUSE, A., LI, Y., STOMMEL, J. M., DELL'ANTONIO, G., MAUTNER, J., TONON, G., HAIGIS, M., SHIRIHAI, O. S., DOGLIONI, C., BARDEESY, N. & KIMMELMAN, A. C. 2011. Pancreatic cancers require autophagy for tumor growth. *Genes Dev,* 25**,** 717-29.

YANG, X. J. & SETO, E. 2007. HATs and HDACs: from structure, function and regulation to novel strategies for therapy and prevention. *Oncogene,* 26**,** 5310-8.

YUAN, Z. L., GUAN, Y. J., CHATTERJEE, D. & CHIN, Y. E. 2005. Stat3 dimerization regulated by reversible acetylation of a single lysine residue. *Science,* 307**,** 269-73.

ZAMARIN, D. & WOLCHOK, J. D. 2014. Potentiation of immunomodulatory antibody therapy with oncolytic viruses for treatment of cancer. *Molecular Therapy — Oncolytics,* 1**,** 14004.

9. Publication List

ELLERHOFF, T. P., BERCHTOLD, S., VENTURELLI, S., BURKARD, M., SMIRNOW, I., WULFF, T. & LAUER, U. M. Novel epi-virotherapeutic treatment of pancreatic cancer combining the oral histone deacetylase inhibitor resminostat with oncolytic measles vaccine virus. Int J Oncol. 2016 Aug 31. doi: 10.3892/ijo.2016.3675. [Epub ahead of print]

10. Erklärungen zum Eigenanteil der Dissertation

Die Arbeit wurde in der Medizinischen Universitätsklinik, Abteilung für Innere Medizin I, unter Betreuung von Herrn Prof. Dr. U.M. Lauer durchgeführt.

Die Konzeption der Studie erfolgte durch Herrn Prof. Dr. U.M. Lauer in Zusammenarbeit mit Frau Dr. S. Berchtold (Laborleiterin und wiss. Mitarbeiterin).

Sämtliche Versuche - mit untenstehenden Ausnahmen - wurden (nach Einarbeitung durch Frau I. Smirnow, MTA) von mir eigenständig durchgeführt.

Der RT-qPCR-Versuch (Results, 3.3), wurde in Kooperation mit Frau Dr. Tanja Wulff (4SC AG, Planegg-Martinsried) durchgeführt. Dabei wurde die Generierung der mRNA-Isolate von mir in Tübingen durchgeführt, die Auswertung der Expressionsrate erfolgte anschließend von Frau Dr. Wulff in München.

Frau Dr. Berchtold hat die Daten für einen Teil der Western Blots (Figures 31 und 33) generiert.

Die statistische Auswertung erfolgte selbständig durch mich (nach entsprechender Beratung durch das Institut für Biometrie).

Ich versichere, das Manuskript selbständig (nach Anleitung durch Frau Dr. S. Berchtold und Prof. U.M. Lauer) verfasst zu haben und keine weiteren als die von mir angegebenen Quellen verwendet zu haben.

Tübingen, den